Effects of the 2018 drought on mire productivity in Skogaryd - Evaluation of ground sensors, satellite data and meteorological data

Inês Júlio Alfredo

2021

Department of

Physical Geography and Ecosystem Science

Lund University

Sölvegatan 12

Inês Júlio Alfredo (2021).

Effects of the 2018 drought on mire productivity in Skogaryd- Evaluation of ground sensors, satellite data and meteorological stations

Master Degree thesis, 30 credits in Masters of *Geomatics*

Department of Physical Geography and Ecosystem Science, Lund University

Level: Master of Science (MSc)

Course duration: *September* 2020 until *January* 2021

Effects of the 2018 drought on mire productivity in Skogaryd - Evaluation of ground sensing sensors, satellite data and meteorological data.

Inês Júlio Alfredo

Master thesis, 30 credits, in *Master's Program in Geomatics*

Supervisors:

Virginia Garcia Millan

Department of Physical Geography and Ecosystem Science,

Lund University

Exam committee:

Martin Berggren

Helena Elvén Eriksson

Department of Physical Geography and Ecosystem Science,

Lund University

Contents

List of Figures

List of Tables

List of Abbreviations

EVI-2	Two-band version of Enhanced Vegetation Index
EEA	European Environment Agency
ESA	European Spatial Agency
FAO	Food and Agriculture Organization
GCS	Geographic Coordinate System
LAI	Leaf area index
MSI	Multispectral Instrument
mV	Millivolt
NIR	Near Infrared
NDVI	Normalized Difference Vegetation Index
P	Precipitation
PRI	Photochemical Reflectance Index
R	Red
RH	Relative Humidity
RMSE	Root Mean Square Error
SITES	Swedish Infrastructure for Ecosystem Science
SWIR	Shortwave Infrared
SIC	Satellite Imaging Corporation
SRC	Skogaryd Research Catchment
TA	Air Temperature
UTM	Universal Transverse Mercator
VIs	Vegetation Indices
WGS84	World Geodetic System

Abstract

In the summer of 2018, Sweden was hit by a long-lasting drought that strongly affected the Swedish nature. The purpose of this study was to examine how drought affected the mire in southwest Sweden located in Skogaryd. Satellite-based remote sensing was used to calculate Normalized Difference Vegetation Index (NDVI) and Two-band version of Enhanced Vegetation Index (EVI2). Time series of these VIs values derived from ground sensors and Sentinel 2 over the months of growing season, for the years 2017 to 2020 and climate data for the same period was used to examine the relation between vegetation indices and meteorological variables, such as air temperature, precipitation and relative humidity.

The studied remote sensing parameters indicates that the values of NDVI and EVI2 from Sentinel-2 were generally lower during the summer of 2018 in dry mire and wet mire with NDVI 0.58 ± 0.052 and 0.51 ± 0.03 and EVI2 0.28 ± 0.03 and 0.32 ± 0.05 respectively. If compared to 2017 with NDVI 0.68 ± 0.01 and 0.54 ± 0.05 and EVI2 0.33 ± 0.02 and 0.25 ± 0.01, 2019 with NDVI 0.65 ± 0.08 and 0.69 ± 0.021 and EVI2 0.24 ± 0.03 and 0.40 ± 0.02 and 2020 with NDVI 0.59 ± 0.01 and 0.54 ± 0.014 and EVI2 0.29 ± 0.012 and 0.42 ± 0.02. However, in ground sensor in dry mire, NDVI and EVI2 are higher in 2018 with 0.88 ± 0.02 and 0.54 ± 0.05 if compered to 2019 with 0.86 ± 0.02 and 0.45 ± 0.05 and 2020 with 0.83 ± 0.02 and 0.37 ± 0.05 respectively, but in wet mire, have law NDVI and EVI2 values with 0.41 ± 0.05 and 0.23 ± 0.03 respectively.

The VIs from Sentinel-2 have positive correlation with VIs from Ground sensor ($R^2 > 0.5$ and p-value < 0.001). The NDVI and EVI2 derived from Sentinel 2 at both dry and wet mire did not show a good correlation with meteorological variables ($R^2 < 0.2$ and p-value> 0.01). However, the ground sensor VIs showed more correlation with relative humidity and air temperature in wet mire than in dry mire ($R^2 = 0.47$ and p-value< 0.001). Surprisingly, did not find correlation between rainfall and productivity in both dry and wet mire ($R^2 < 0.3$). In addition, 2019 was a year with high cumulative precipitation (1083.4 mm), refilling the water sources of the mires in Skogaryd.

Keywords: Sentinel 2, VIs, Ground Sensors, Drought and Mire

Acknowledgement

Throughout my course and during the period of preparation of the end-of-course work, I had contributions from several people, including teachers, family, friends and colleagues. With the conclusion of this master dissertation, I would like to thank everyone who helped me achieve my goals.

First, I thank GOD for the powerful and the merciful, for having granted the gift of the life, wisdom and for illuminating life every day. To my parents (Celina Massilela Madal and Julio Libanio Alfredo) special thanks goes out because they gave me life and all the support from the first day of my life until today. I thank my brothers Albano Julio Alfredo, Ricardo Branquinho Madal and Julio Libanio Alfredo Junior and my beloved son Donato Leonardo Cristovao for the support and love dedicated to me during my life.

To the Department of Mathematics and Informatics of Eduardo Mondlane University, to all teachers in particular to (Dr. Marcio Mathe and Dr. Antonio Assane), who directly or indirectly, helped me during my academic career and the Lund University. To Department of Physical Geography and Ecosystem Science for their support during the master's course and access to the workstation for data processing.

1. Introduction

Drought is a complex meteorological phenomenon associated with low precipitation and low water saturation in atmosphere, soils and plants (Wilhite et al. 2000). It has a great effect on aboveground biomass and, if severe, can change the structure and function of forest ecosystems (Allen et al. 2010). Drought is a natural disaster that causes significant environmental, economic and social impacts (Kelman et al. 2016). According to Below et al. (2007), drought is one of the most significant hydro-climatic hazards striking the environment and society. However, it is not easy to quantify its effects, as the start, end, duration, intensity and spatial extent of a drought episode are not easy to determine (Wilhite et al. 2000). Generally, the most prominent types of droughts are meteorological, agricultural, and hydrological droughts (Wilhite, 2000). In the analyses of droughts, their onset, duration, and severity are often difficult to determine and the characteristics may vary significantly from one region to another (Rulinda et al., 2012).

The drought facilitate the spread of plant plagues and diseases (Rosenzweig et al. 2001) and induces tree and pasture mortality (Allen et al. 2010). The droughts also are known to reduce the primary and secondary productivity of vegetation (Bennett et al. 2015). The vegetation productivity indicates the spatial distribution and change of vegetation cover on the ecosystem (EEA, 2020). The Climate has high influence on vegetation productivity, which the strongest driver is precipitation (EEA, 2020). The precipitation is a very relevant variable for plant-atmosphere system, because water in the soil is consumed partly by evaporation from the soil and partly by the transpiration of plants and its deficits can lead to reduced photosynthetic capacity and changes in absorption of solar radiation in photosynthetically active radiation by plants (Davidson and Janssens, 2006).

The global increases of mean temperature mainly caused by emissions of greenhouse gases are widely acknowledged by the scientific community (Stephenson, 2008). Further increases of mean temperature are expected in the future, with higher frequency and severity of extreme drought events and heat waves and related impacts and damages (IPCC, 2007). Plants pass through a series of morphological, physiological, biochemical and molecular changes in order to mitigate these adversities from abiotic stresses such as water deficit (Anjum et al. 2017). The drought stress in plants reduce the leaf water potential and turgor pressure, which makes living plant tissues rigid, Loss of turgor, resulting from the loss of water from plant cells, causes flowers and leaves to wilt

(Farooq et al., 2009). Stomata closure, and decreased cell growth influencing biochemical functions such as photosynthesis, chlorophyll synthesis, nutrient metabolism, respiration, and carbohydrates metabolism (Li et al., 2011; Farooq et al., 2009b). The actual climate scenario is playing an important role in changes in vegetation productivity (Vicente-Serrano et al. 2014; Ciais, 2005).

The mire ecosystem are highly integrated ecosystems which are vulnerable natural and human induced perturbations, are dominated by direct and indirect effects of climate change arising from global warming, which has multiple implications for Arctic peatlands (Minayeva et al. 2010). During droughts episodes, mires ecosystems show resilience to limited water availability due to their plant species either being tolerant to drought, are able to reestablish when wet conditions return (Capon, 2003). The Vegetation productivity is easily studied over the areas using remote sensing spectral vegetation indices, such as the normalized difference vegetation index (Tucker, 1979) and the enhanced vegetation index (Huete et al. 2002). Satellite remote sensing has been employed to study the effects of disturbances on ecosystems with vegetation indices, which capture spectral changes caused by changes in vegetation physiology (AghaKouchak et al. 2015; Walker et al. 2011).

Remote sensing observations have been used to monitor drought related with meteorological variables and also to assess and quantify drought impacts from an ecosystem (Sorooshian et al. 2011; Entekhabi et al. 2004; Cashion et al. 2005). Combinations of satellite visible and infrared images have been widely used to monitor plant changes and water stress (Gu, et al. 2007). Quantified 2018 drought impacts in various European countries using satellite images and meteorological data (Allan Buras et al. 2019; Flink and Stålnacke 2019).

The summer of 2018, Europe experienced an exceptional drought and heatwave, also affecting Fennoscandia mire and forest ecosystems (Linderson et al. 2020). Vegetation indices has been widely used in remote sensing as an effective indicator of plant growth to examine the spatial and temporal patterns of vegetation greenness and productivity and their responses to climate change (Zhang et al. 2014). The frequency of droughts in Europe in the last years and particularly in Northern ecosystems, has motivated the interest in studying the impact of 2018 drought in Skogaryd using satellite data, ground sensor and meteorological data (TA, P and RH).

Other studies quantifies the drought in various European countries in different periods of time, such as the heat wave and drought episode experienced during summer 2003 (Dotzler et al. 2015; Reichstein et al. 2007; Ciais, 2005; Rennenberg, 2006), the drought occurred in 2010 (Cherenkova, 2013) and the extreme drought event occurred in summer 2017 (Puletti et al. 2019). However, to our knowledge, no study so far has explicitly investigated differences in drought resistance between wet mires and dry mire ecosystem productivity with VIs and meteorological data. One side, there is possibility that wet mires are more resilient to drought because there is more water available and the plants can afford evapotranspiration of part of the water table, if the drought is not very long. However, it can also happen that the species in the wet mire are more sensitive to changes in water availability and they will suffer more than species from a dry mire, in a drought event. About the dry mire, is expected to study if the plants will suffer greatly from drought because there is not so much water available, or if the species on the dry mire are more resilient to drought. In this study, using ground spectral sensors and Sentinel 2 data for characterization of drought impacts on vegetation, taking the year 2018 as a reference for drought.

2. Aim

The main aim of this study is how did the change of temperature (TA), relative humidity (RH) and precipitation (P) in summer 2018 affect the vegetation productivity on mire ecosystem, for which following questions are addressed:

1) Are the NDVI and EVI2 derived by satellite images and ground sensor data correlated with meteorological data?

2) Are NDVI and EVI2 from Sentinel-2 correlated with the similar VIs from ground sensor data?

3) Is dry mire more drought-resistant than wet mire?

3. Background

3.1 Climate change and its impact on mire ecosystem

Mire ecosystems are defined as wetlands with vegetation, which usually forms peat (or litter) that has not completely decomposed and has accumulated because of anaerobic conditions connected with a high water table (Mezbahuddin et al. 2013). The peat formation is possible where the water table is close to the surface for most of the time (Rydin et al. 1999). Mires are highly- integrated ecosystems that are vulnerable to natural and human induced perturbations, including direct and indirect effects of climate change, which has multiple subtle implications for peatlands (Minayeva et al. 2017). Mires are predominantly northern ecosystems, especially abundant in continental boreal and sub-arctic regions, but they are also found in the tropics (Lappalainen, 1996). The occurrence of mires and peatlands are strongly related to topography, with the greatest abundance found on flat land areas (Lappalainen, 1996). The distribution of mires over the globe clearly reflects their dependence on climate (Minayeva et al. 2017). As mires are mainly concentrated in humid or cool regions, a changing climate is expected to affect their carbon balance and radiative forcing (Grip and Rodhe 1994). Since net primary production and decomposition are closely related to moisture and temperature, significant alterations in the carbon dynamics of peatlands may result from climate changes (Galambosi et al. 2000). Some researchers mention the importance of changes in the water table level, which can increase the accumulation of carbon in the northern mires, but can create a larger source of carbon dioxide in the southern mires (Richardson et al., 2013). Others authors argue that an increase in temperatures can lead to a loss of net carbon in southern mires, but a net carbon gain in northern mires (Lappalainen, 1996).

Climate change affects the physiological processes of ecosystems and, therefore, changes their phenology, photosynthetic capacity and respiration, as well as the availability of soil nutrients (Richardson et al., 2013; Hänninen & Tanino, 2011; Ågren et al., 2008). There is substantial uncertainty regarding future weather conditions.

3.2.   Vegetation Indices

Spectral Vegetation Indices are a mathematical combination of spectral bands that highlight the spectral properties of green plants so they can be distinguish from other features, such as soil, snow, water or dry vegetation (Zhang et al., 2019). Many vegetation indices are calculated by combining the red spectral band with the near-infrared band, to highlight the slope in green vegetation spectral signature, between the red and near-infrared bands (AghaKouchak et al. 2015). This slope, called red edge, is characteristic of green vegetation because plant pigments such as chlorophyll, anthocyanin, or carotenoids in the photosynthesis mostly absorb visible light, while plants by the water contained in the mesophyll, to control the plant temperature (Rondeaux et. al 1996), mostly reflect the infrared light. For this study, was used two spectral vegetation indices for observing vegetation greenness, was applied NDVI (Walker et al., 2011) and EVI-2 (Jiang et al. 2008).

NDVI is one of the most used vegetation indices in biomass estimation, plant health leaf area index and plant productivity (Peters et al. 2002). This VIs is calculated based on amounts of light reflected by growing vegetation registered by satellite sensor near infrared (NIR) and red (RED) bands as in equation 1 (Rouse, et al. 1974). The NDVI and EVI2 range between -1 and 1. The higher value means that the vegetation is healthy, or the biomass is high, or the productivity is high (Jackson and Huete 1991). While lower values means dry vegetation, snow, water, clouds or soil absorb considerably more of NIR (Myneni et al. 1995).

The limitation of NDVI is that it saturates at biomes with the highest LAI values, on tree plantations, temperate evergreen forests, and wetlands (Scurlock et al., 2001). Therefore, an alternative VI, designed to minimize the influences of soil and aerosols and to solve the problem of saturation in dense is EVI, this VI is commonly used as an alternative to NDVI in regions with high biomass (Jiang et al. 2008). EVI has since been developed in a two-band version called EVI2 (Table 1), this no longer incorporates the blue band (Jiang et al. 2008). 2-band of EVI (EVI2) was developed for sensors with no blue band, such as MODIS (Jiang et al. 2008).

Table 1: Vegetation Indices

Vegetation Indices	Formulas	Source
NDVI (1)	$$\frac{NIR - Red}{NIR + Red}$$	(Rouse, et al. 1974)
EVI2 (2)	$$2.5 * \frac{NIR - Red}{NIR + 2.4 * Red + 1}$$	(Jiang et al., 2008)

Where in EVI2 Value 1 is the soil adjustment factor and 2.5 correspond to a gain factor, and 2.4 used to reduce soil background effects.

Both NDVI and EVI2 have been used in several studies to quantify the stress of vegetation and the impacts of drought in Europe (Reinermann et al. 2019). The spectral vegetation indices have been used in applications such as agriculture and forestry (Zhang et al., 2014) also to estimate crop biomass. Because it is already known that with the photosynthetic capacity compromised, the absorption of solar radiation by the leaves at photosynthetically active wavelengths decreases and more radiation is reflected, reducing the contrast between R and NIR (AghaKouchak et al. 2015). In those studies were used the MODIS EVI time series to quantify the spatial-temporal variability in drought impacts in Germany, investigating EVI anomaly patterns for different types of land cover and comparing droughts in 2003 and 2018. The study conclude that, although the phenology of spring 2018 was above average, both years showed negative summer anomalies of similar magnitude, with grasses and agricultural areas the most affected. In other hand, were not found negative anomalies for forested areas for 2018 due to its ability to reach deeper ground water.

3.3. Spectral reflectance of mire ecosystems

Mire is a type of wetland with a vegetation, which usually forms peat that is sensitive to changes in water conditions and is thus a good indicator of changes in water supply over a long period of time (Bubier, Rock & Crill, 2005). Due to this sensitivity, studies on the spectral reflectance of the moss are advantageous for examining the water status of a wetland (Bubier, Rock & Crill, 2005). On the other hand, mapping wetlands on a larger scale can be a difficult task because wetlands

usually do not consist of a certain amount of water or homogeneous type of vegetation, which results in a high variation of spectral reflectance depending on which wetland is, studied (Töyrä & Pietroniro, 2005). The Shortwave Infrared bands are suitable for characterizing vegetation on mires, as the bands are sensitive to moisture present in both soil and vegetation. Changes in the hydrology of a bog therefore have a major impact on the efficiency of photosynthesis (Davidson and Janssens, 2006).

The type of vegetation of the mires are sensitive to temperature, increasing temperatures may increase the microbial heterotrophic respiration, and consequently lead to increase CO_2 fluxes to the atmosphere, which in turn would accelerate the temperature rise with can effect on the soil respiration (Heimann and Reichstein, 2008; Schlesinger and Andrews, 2000). The low relative humidity when the air outside the leaves is very dry and the increase of temperature will increase respiration, which in turn will increase the internal CO_2 concentration in the leaf, which will cause the stomata to close (Willmer and Fricker, 1996; Monteith, 2000) to prevent desiccation.

This reduces the intake of CO_2, therefore reducing photosynthesis and plant productivity, which can be observed in changes in reflectance, when plants are not doing photosynthesis and they reflect more the visible light. NDVI (Huete et al., 2002) is based on the change of slope between red and near infrared bands (red edge). A reduction in photosynthesis involves a reduction in the red edge slope, and therefore, a reduction on NDVI values (Carlson and Ripley, 1997).

3.4. Satellite remote sensing - Sentinel 2

Sentinel-2 is part of Copernicus, a satellite program administered by European Space Agency (ESA), Sentinel-2 is a collective name for two satellites, Sentinel 2A, which was sent up in 2015, and Sentinel 2B, which was sent up in 2017(SIC, 2016). One purpose of the program is to monitor land use changes on Earth (Puletti et al. 2019). This multispectral satellite collect data by carrying a multispectral imager instrument, a passive sensor that measures the Sun's radiation reflected by the Earth in 13 bands of different wavelengths, within 5 days visit time (Reese & Olsson, 2018). Of these bands, 4 bands are visible, 6 bands are Near-Infrared, and 3 bands are Short-Wave Infrared. The Sentinel-2 satellite images are composed of 100*100 km^2 tiles (orhto-images with UTM, WGS84 projection) (SIC, 2016).

Since Sentinel-2 consists of two satellites with 290 km wide stage size, there are now good opportunities to get high-resolution images of specific geographical areas (Reese & Olsson, 2018). The launch of the Sentinel satellites has changed research and had increased opportunities for studies, combining a frequent revisit, a large swath, and systematic acquisition of land surface images at high spatial resolution, with spectral bands that guarantee consistent time series that can show the variability in land surface conditions and minimizing the atmospheric affects (Puletti et al. 2018). Moreover, Sentinel 2 has the potential to monitor the health condition, growth, and productivity of terrestrial ecosystems at a wider and local scale (Dotzler et al. 2015). The Table 2 shows the description of bands of Sentinel-2 and respective spatial resolution used in this study (SIC, 2016).

Table 2: Sentinel-2 band, wavelength and resolution of the pixel for each band

Sentinel-2 Bands	Central Wavelength (µm)	Resolution(m)
Band 1 -Coastal aerosol	0.4436	60
Band 2 -Blue	0.4901	10
Band 3 –Green	0.5601	10
Band 4 –Red	0.6651	10
Band 5 -Vegetation Red-edge1	0.7052	20
Band 6 -Vegetation Red-edge2	0.7402	20
Band 7 -Vegetation Red-edge3	0.7832	20
Band 8 -NIR	0.8421	10
Band 9 -Water Vapor	0.9456	60
Band 10 -SWIR –Cirrus	1.3756	60
Band 11 -SWIR	1.6102	20
Band 12 -SWIR	2.1902	20

3.5.   Ground VIs

The ground raw spectral data are averaged in the data logger into 10-minute intervals. The Quality control is done by visual check and automated range check to identify outliers and erroneous data.

Currently a database system with web interface for database storage, management (quality control, display, computation of vegetation indices, data export. The VIs from ground sensor are computed after he data be calibrated. With have some calibration certificates, from which got a calibration

factor (k), for each band then multiply each band by that k-factor, then the data is calibrated each band (Sites, 2018). The computation of spectral vegetation indices were done by equation 1 and 2.

The VIs are from sentinel 2 and from ground sensor that are relatively the same but they differ with pixel size, and therefore, what plants fall within one pixel, there is the full atmosphere between the satellite and the ecosystem while the ground sensor there is only few meters of atmosphere between the sensor and the vegetation. That can add noise to the VIs from satellite, even though was performed an atmospheric correction.

4. Data and Methodology

4.1. Study Area

Skogaryd, located 100 km north of Gothenburg, located at approximately 80 meters above sea level is an area of approximately 1000 hectares (58 ° 23′N, 12 ° 09′E) (Klemedtsson et al., 2010). The station has been part of SITES since 2013, which is a nationally coordinated infrastructure for land and water-based research.

Skogaryd research area consists of six sub-areas; clear-cut on pododzol soil (Stordalen), the lakes Ersjön and Följesjön, forest on drained organic soil, forest on mineral soil (Central) and the Mycklemossen mire (bog) (Klemedtsson et al., 2010).

Skogaryd was chosen as a study area as it is a well-documented area with good infrastructure for research and contains vegetation types that are typical of large parts of southern Sweden's landscape (Banzhaf, 2015). This study will focus on the mire ecosystem (figure 1).

4.1.1. Mycklemossen Vegetation

The vegetation at the mire ecosystem in Mycklemossen can be classified as Hare's-tail Cotton grass-Sphagnum rubellum type or Heather-Sphagnum rubellum type (figure 2) according to Påhlsson (1998). The vegetation is quite homogenous across the mire ecosystem, which is composed of a mosaic of drier hummocks and wetter hollows. The hummocks are dominated by Eriophorum vaginatum and dwarf shrubs such as Calluna vulgaris and Erica tetralix while the hollows are characterized by different Sphagnum species, mainly S. rubellum, S. fallax and S. austinii, and Rhyncospora alba. Towards the centre of the mire, conditions are drier and the vegetation is more forest-like, with a sparse tree layer dominated by Pinus sylvestris, and more dwarf shrubs such as Vaccinium uliginosum, V. myrtillus and V. vitis-idaea.
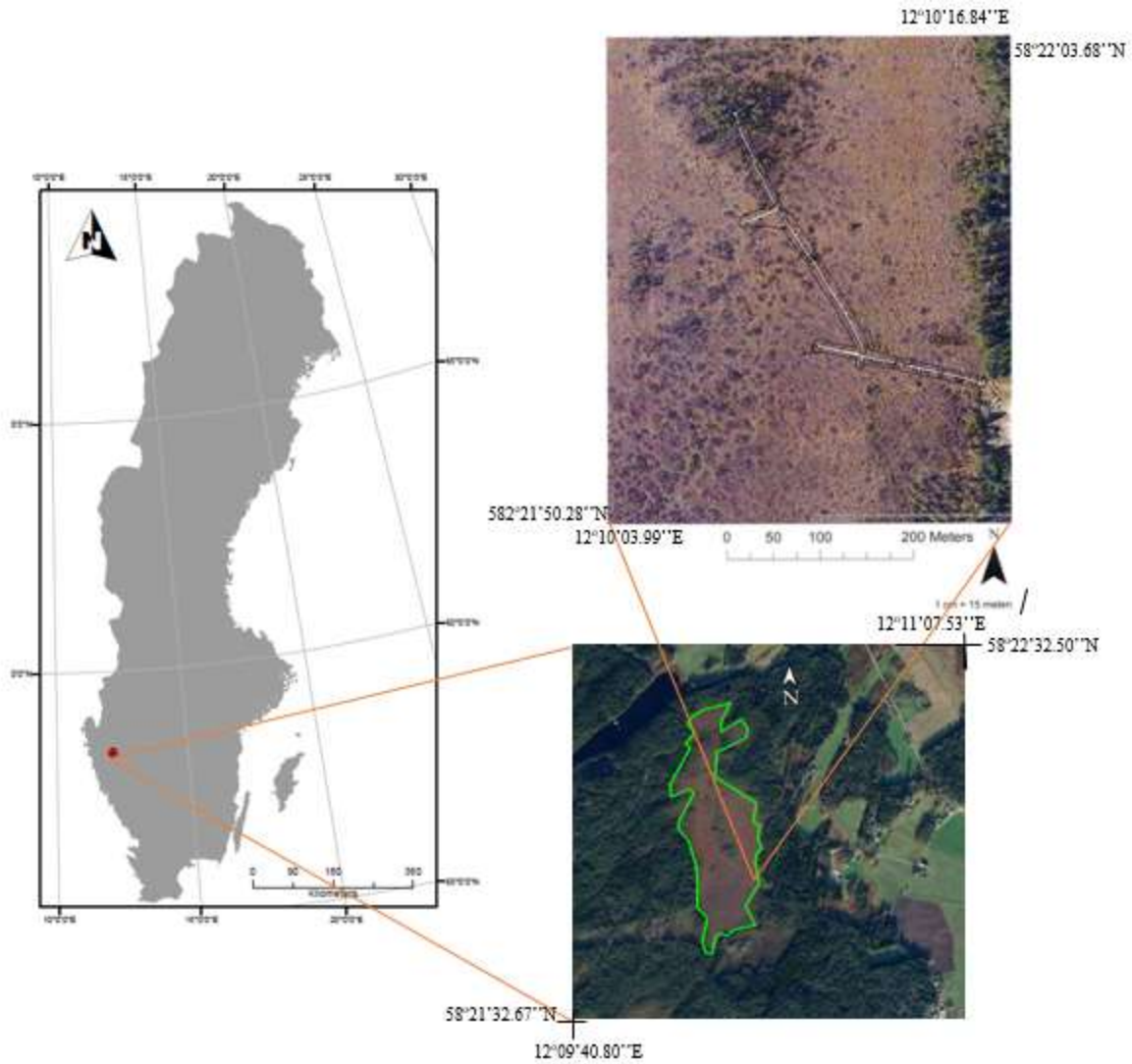
Figure 1: Skogaryd Research Area, in Southwestern Sweden, the study site is mire (MYC) (shown in the zoomed in google earth). The administrative boundary data from DIVA-GIS (2019). The projected coordinate system is SWEREF99TM.

a)   b)

Figure 2: The dry mire ecosystem characterized with no water in surface a) and wet mire ecosystem with water in the surface b). Source (Sites, 2018)

4.2. Datasets

For the development of this thesis, three datasets were used spectral ground sensor data, meteorological data and satellite data. The spectral ground data consists of a time series of multispectral sensors from MYC, from years 2017 to present (SRC, 2020). In addition, a meteorological dataset has been used, located at MYC, from 2017 to 2020 (SRC, 2018; SRC, 2020; SRC, 2021). These two dataset belong to Skogaryd station, and it is managed by the SITES Spectral project with PID 2017 (11676.1/gFHqMeAdP bHjsxvYi7nLWHC0), 2018 (11676.1/nlP1-wHXFPkO8VJXjxSbilvc), 2019 (11676.1/CzQ1X RzyCqprClwU18i5vH2c) and 2020 (not published). The used satellite data is from Sentinel 2, which carries a multispectral sensor, and is part of the Global Monitoring for Environmental and Security program (GMES), in partnership with European Space Agency (ESA) (EO, 2016). The spatial resolution is 10 m, 20 m or 60 m, depending on wavelength (Table 1) (SIC, 2016). The images can be freely acquired and accessed online in ESA Copernicus Sentinels Scientific Data hub website.

4.2.1. Sentinel 2 images

The Sentinel 2A products are available to users in Level-1C and Level-2A. MSI level-1C were used in this thesis, which is a high-resolution multi-spectral imaging mission for many applications, including land monitoring, emergency response and security services assistance (ESA, 2017). The Level-1C is Top-Of-Atmosphere (TOA) reflectance in fixed cartographic geometry. This level of processing includes radiometric and geometric corrections as Orth-rectification and spatial registration on a global reference system (UTM projection and WGS84 ellipsoid) and images are a set of tiles of 100 sq. km (Drusch et al., 2012).

The Sentinel-2 products are in Sentinel-SAFE format that includes image images in JPEG2000 format, quality indicators, auxiliary data, and metadata. The SAFE data folder contains image data in binary format and XML metadata. Images at level 1C are processed by the Payload Data Ground Segment (PDGS) distributed online. The Level 1C product results from the use of a Digital Elevation Model (DEM) to project the image in cartographic geometry; it contains Top Of Atmosphere reflectance (TOA) per pixel containing the parameters to transform them into radiance. Level 2A products are generated from users based on Level 1C products using Sentinel-2A tools that convert reflectance from the top of the atmosphere to the bottom of the atmosphere (BOA) in cartographic geometry. Level 1C products, the pixel coordinates are referenced to the top left corner of the pixel (ESA, 2017).

Sentinel-2 was considered suitable for this research since it has a high spatial resolution of 10 m for the red (band 4) and NIR (band 8) channels, which are used for the calculation of NDVI and EVI2. The acquisition dates of the images were since 2017 to 2020, on the period between April to October, one image per month, being a total of 28 images.

The winter months were excluded because of the difficulty to find cloud or snow free in the images. The figure 3 below illustrate the temporal distribution of the images in dates of acquisition
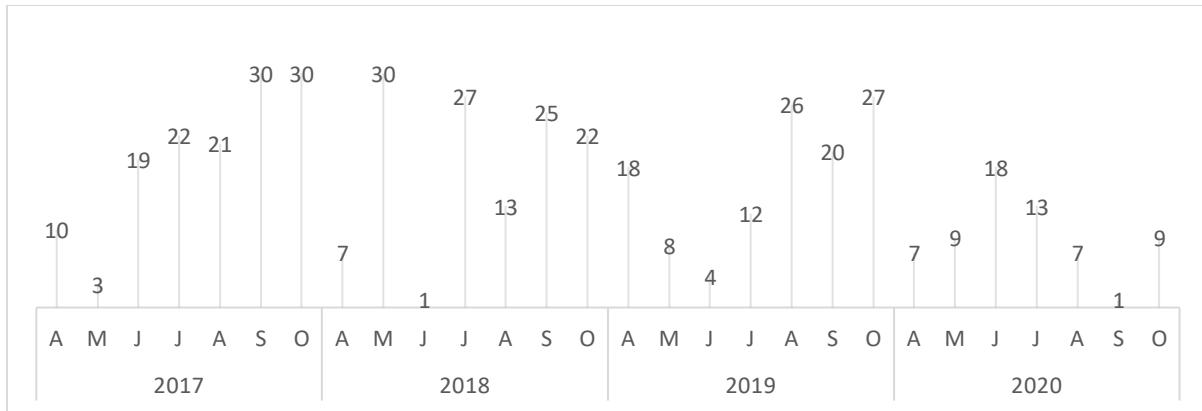
Figure 3: Selected dates for Sentinel-2 satellite images used in the study for 2017 to 2020 from April to October. The images were acquired online from ESA Copernicus Sentinels Scientific Data hub website

4.2.2. Ground sensor data

The ground sensor used was multispectral sensors manufactured by Decagon Devices (Pullman, US). The Decagon spectral sensors consists of two-channel sensors for measuring Normalized Difference Vegetation Index (NDVI) or Photochemical Reflectance Index (PRI). The installation of these sensors involves one upward looking to enable hemispherical view, and one downward-looking sensor, with stops in 35° field-of-view (FOV) angle to enable directional conical view. Decagon sensors measure the sun radiance (W/m2 * nm) and ground irradiance (W/m2 * nm * sr). The light collected from the sun is used to calculate the reflectance of the observed ecosystem, referred to as the ratio of the reflected light from the vegetation, from the total amount of light that arrived to the ground surface (SITES, 2018).

Continuously measured ground multispectral data at Skogaryd mires were used in this research, to make comparison between ground multispectral vegetation index and vegetation index time-series reconstructed from Sentinel-2 data. In Mycklemossen, a pair of Decagon SRS-NDVI sensors and a pair of Decagon SRS-PRI sensors are located at 4.5 m above the ground, looking at a dry mire (Northwest orientation). Another set of NDVI/PRI sensor is also located at 4.7 m, looking at a wet mire (North orientation) (SITES, 2018). In this study, was used only the NDVI sensor because Sentinel-2 does not have the bands to calculate PRI. These Decagon sensors were installed in 2017. Table 2 summarizes the ground sensor set-up of the studied areas.

Table 3: The Decagon NDVI Ground sensor parameters used in Mycklemossen, Skogaryd. (SITES,2020)

Coordinates (WGS84)	Sensor type and brand	Bands (nm)	Field of View (FOV, degrees)	Units	Ecosystem	Set-up (height & orientation)
58.382N 12.146E	Decagon -NDVI	650 (Red) 810 (NIR)	180° (Up) 36° (Dw)	$W*m^{-2}*nm^{-1}$ (Up) $W*m^{-2}*nm^{-1}*sr^{-1}$ (Dw)	Wet mire	4.7 m 0° (N)
					Dry mire	4.5 m 290° (NW)

4.2.3. Meteorological data

The raw meteorological data in Mycklemossen is collected every 30 min, continuously. The weather stations collect air temperature, relative humidity, air pressure, wind speed, wind direction, incoming and outgoing shortwave radiation, incoming and outgoing longwave radiation, albedo, and snow depth. For this study, were only used air temperature, precipitation and relative humidity data over the years (2017 to 2020) from Skogaryd Research Catchment station, in Mycklemossen (58.364943N, 12.169817E).

The distance between ground sensor station and meteorological station is 2.3 kilometers as represented in the figure 4 bellow.
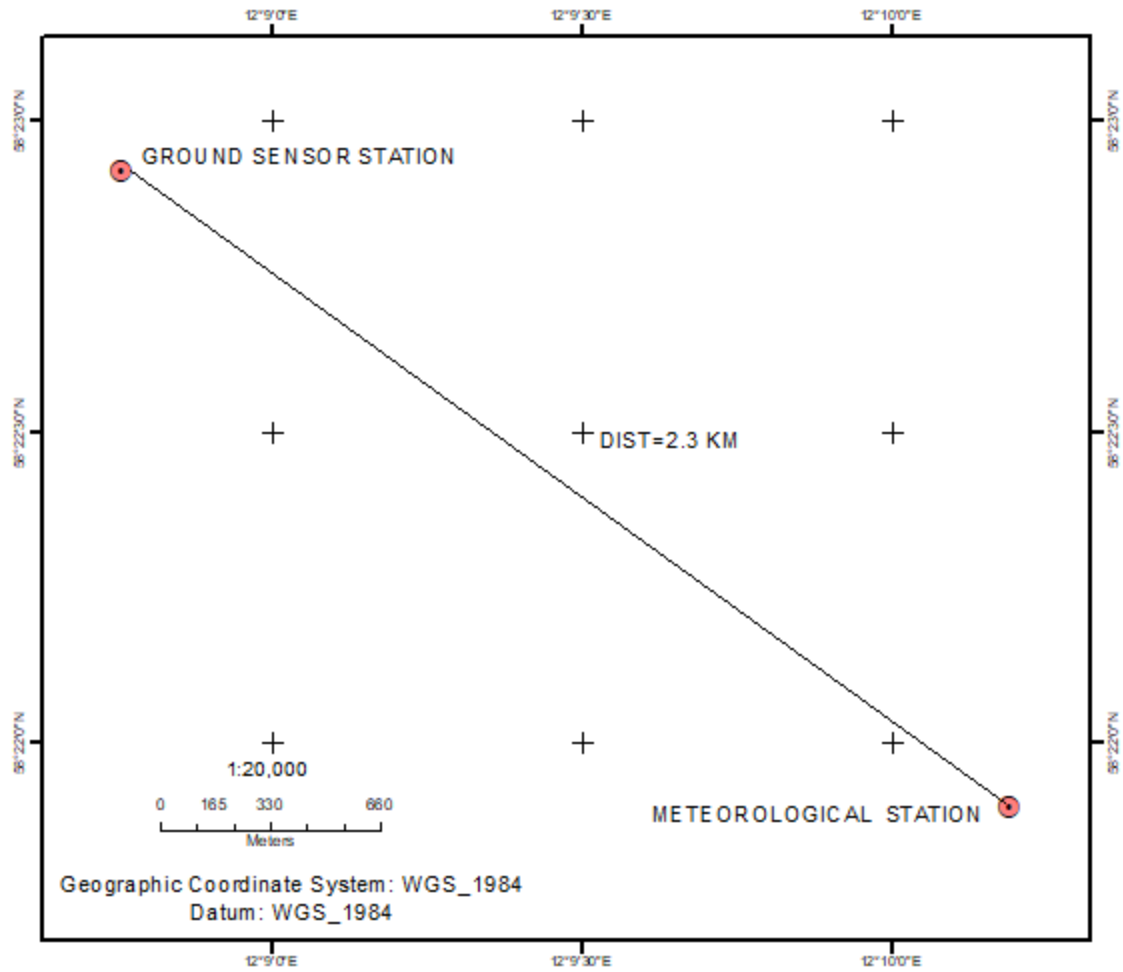
Figure 4: Representation of location of meteorological station and ground sensor station and the distance between them (SRC, 2020).

4.3. Methodology
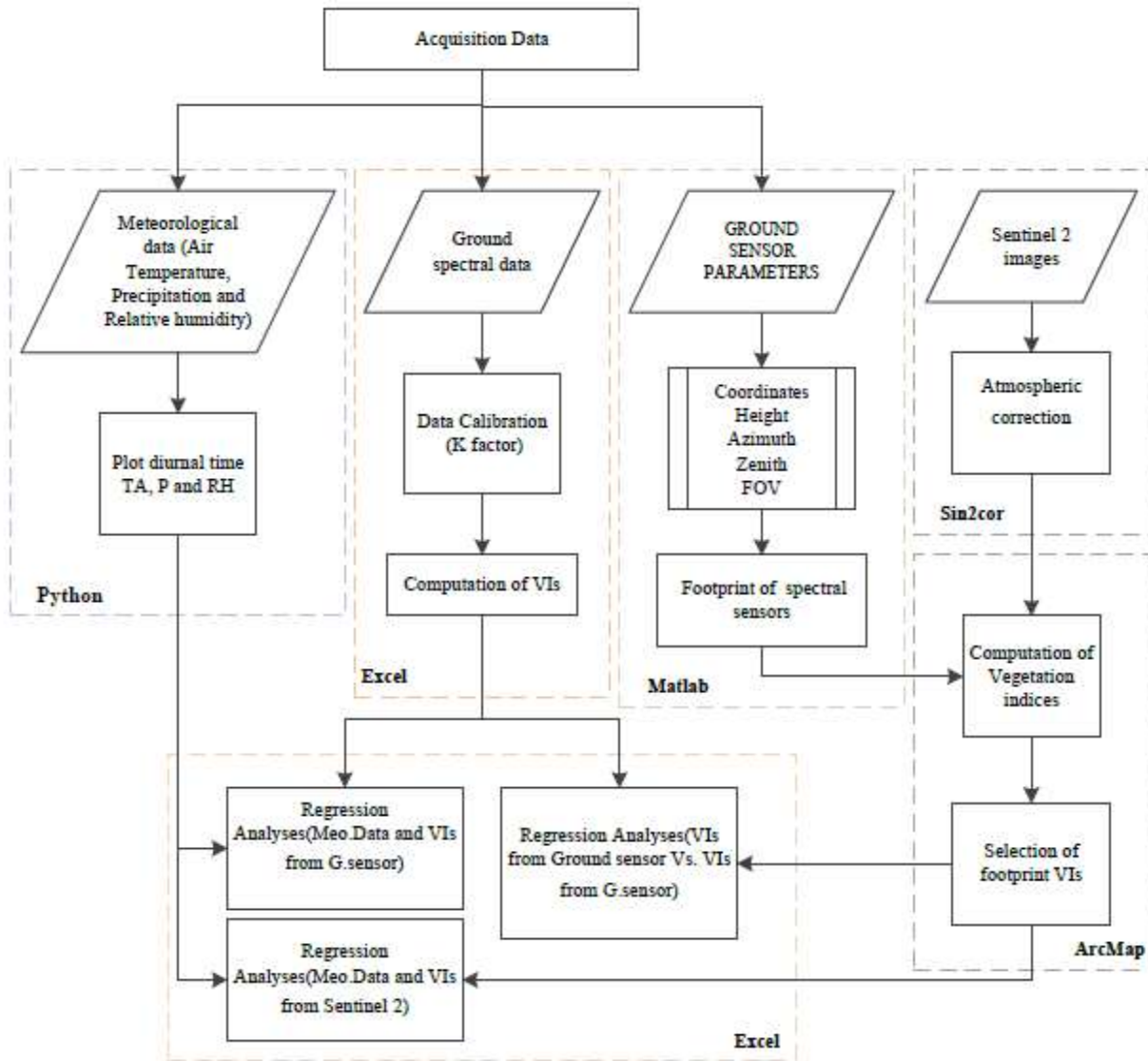
Figure 5: The workflow of the research method where the arrows show the sequences of process steps, dashed lines divide the methodology in steps, the rhombus mean input data, squares mean process and the square with two vertical lines inside means input variable (parameters).

The workflow of the research method is depicted in diagram as shown in figure 5 above. This is the combined steps processing to achieve the objective of the current research: data collection, data processing, inter-comparison of those results.

4.3.1. Data Processing

4.3.1.1.Meteorological data processing

For the purpose of this study, air temperature (TA), Precipitation (P) and relative humidity (RH) were plotted for diurnal time (9 a.m. to 2 p.m.) and averaged from 30 min to daily measurements. For this task was used Python 3.8. The meteorological data were used to confirm the drought in 2018 in Skogaryd and evaluate if this variables affect the vegetation productivity of mire ecosystem.

4.3.1.2.Ground sensor data processing

The raw data were first calibrated using a k-factor provided by the manufacturer of the sensors, which is multiplied, for each band, to the raw radiance and irradiance collected by the ground sensors. Second, reflectance was calculated, as a ratio of the looking-up sensor (sun radiation) and looking-down sensor (vegetation irradiance), per each band. At last, reflectance, per band, were used to calculate the spectral indices NDVI and EVI2.

The footprints of the spectral sensors were calculated in Matlab R2018b, using the sensor height, sensor field-of-view, zenith angle, azimuth angle and geographic (Table 4).

Table 4: The decagon NDVI sensors parameters used to calculate ground sensors footprint. (SITES, 2020)

Ecosystem	Sensors	Coordinates (WGS84)	Sensor height	Field of View (FOV)	Azimuth angle (degrees)	Zenith Angle (degrees)
Dry mire	Decagon sensor NDVI (1)	58.365028 N 12.170711 E	4.5 m	36	0	45
Wet Mire	Decagon sensor NDVI (2)		4.7 m	36	295	45

4.3.1.3. The footprint of dry and wet mires

The figure 6 shows the location of the ground sensor footprints on the mires. The footprints were presented on NDVI Sentinel 2 raster. Both footprint has an area of 23.6 m². The footprint looking to dry mire cover 3 pixels, while the footprint looking to wet mire covers 2 pixels, with 10 m resolution. The NDVI and EVI2 values for Sentinel 2 were extracted for the pixels that coincided with the footprints, and the assigned value was calculated as a weighted average, by multiplying each value of the pixel (P.1, P.2, P.3 and P.4) by its weight (Hu, 2010) considering the area of each pixel that contributed to the footprint area. The weighted average Northwest footprint looking to dry mire (Wdry) and footprint looking to wet mire (Wwet) are calculated using equation 3 and 4 respectively, where the weight should be not negative.

$$Wdry = \frac{w1 * P.1 + w2 * P.2 + w3 * P.4}{w1 + w2 + w3} \qquad equation\ 3$$

Where the w1 = 10, w2 =40 and w3=60

$$Wwet = \frac{w1 * P.2 + w2 * P.3}{w1 + w2} \qquad equation\ 4$$

Where w1=40 and w2 =60
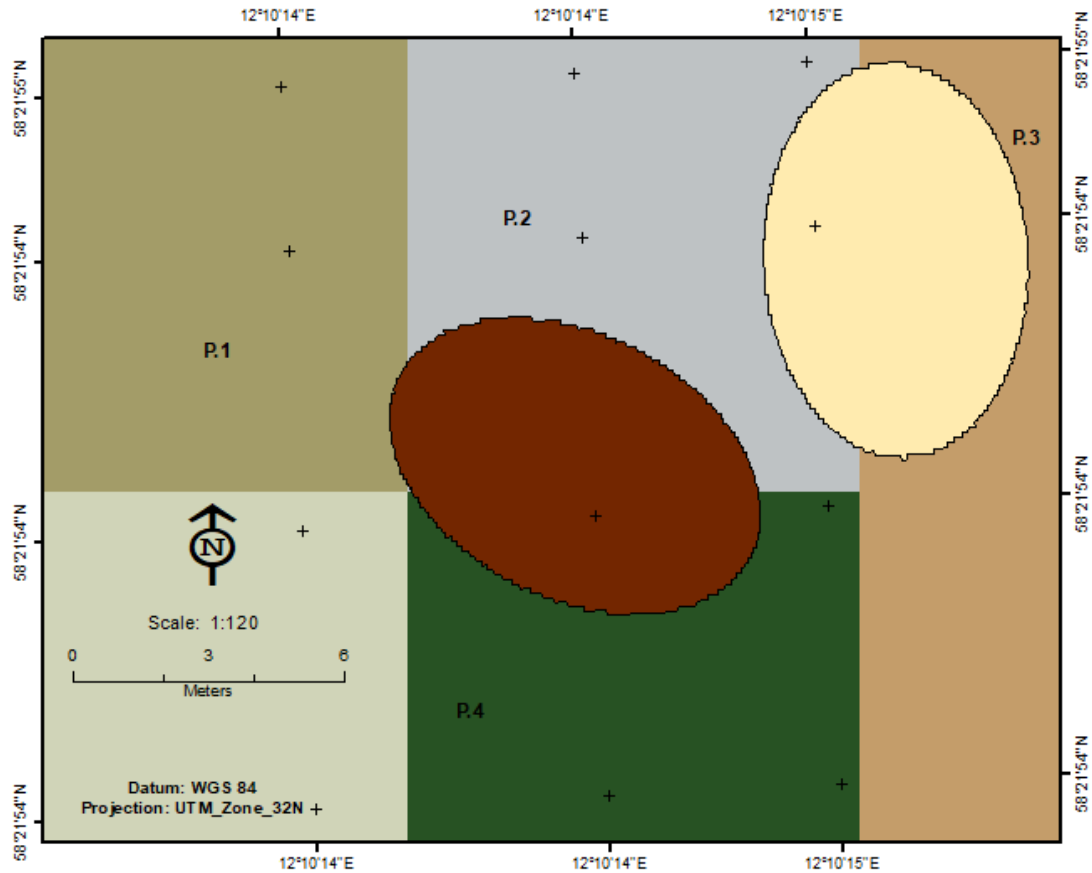
Figure 6: Footprints of NDVI Decagon sensors in Skogaryd Mycklemossen (mire) on Sentinel-2 raster with 10 m resolution. The brown footprint is looking to North West in dry mire and white pink footprint looking up to North in wet mire. The red point is where the tower is located.

4.3.1.4. Sentinel-2 processing

Sentinel-2 Level of processing L1C products provide the top of atmosphere reflectance in fixed cartographic geometry, and the products contain applied radiometric and geometric corrections (ESA, 2017). Then, data ware atmospherically corrected using Sen2Cor processor and SRTM Digital Elevation Model as auxiliary data to improve the terrain correction (ESA, 2020). Once the images were converted into Bottom-of-Atmosphere reflectance, then calculated NDVI and EVI2, using the formulas in equation 1 and 2 described above. Below, in figures 7 and 8, maps for NDVI and EVI2, respectively both vegetation indices were derived from satellite images from ESA (2020).
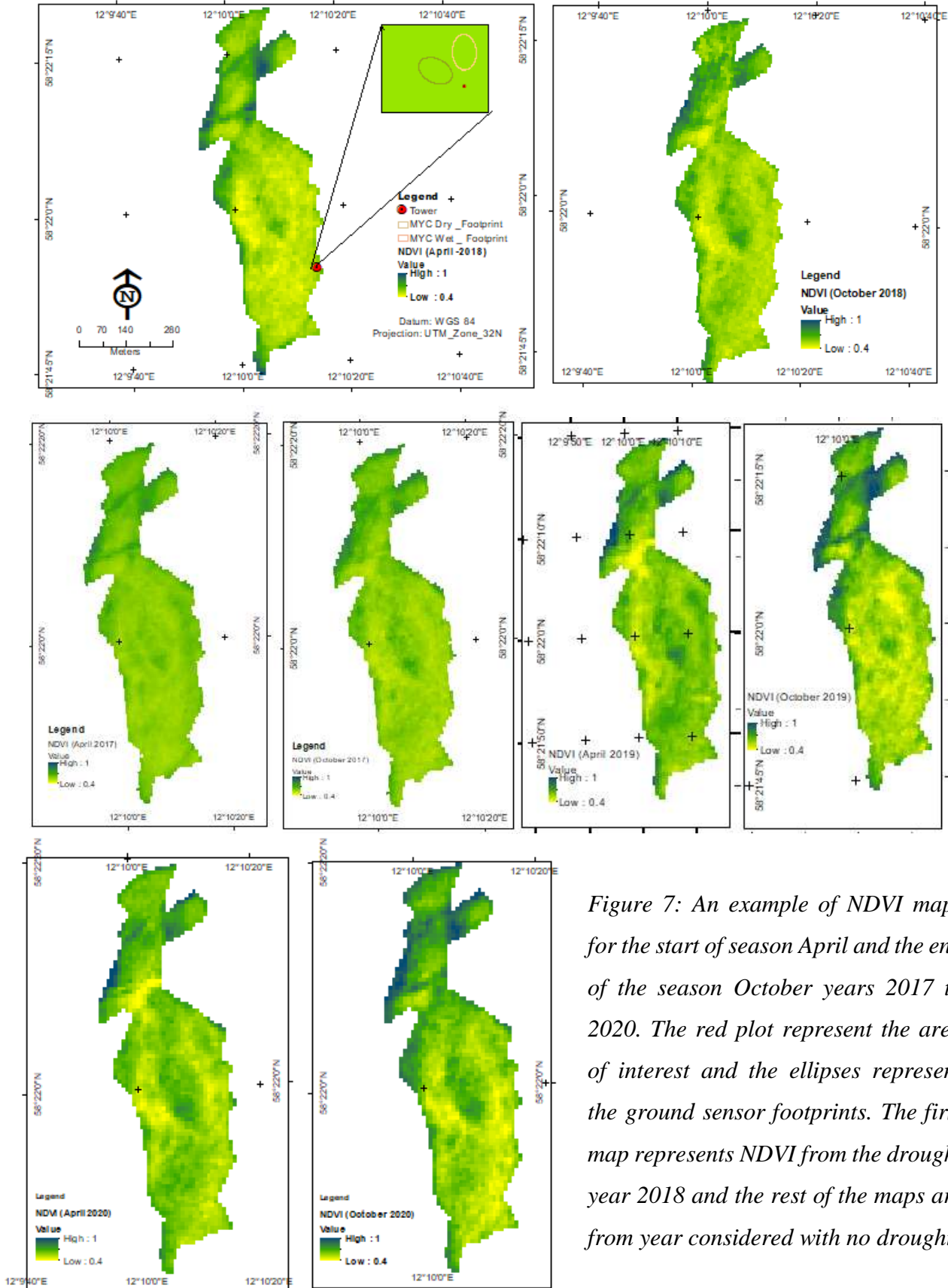
Figure 7: An example of NDVI maps for the start of season April and the end of the season October years 2017 to 2020. The red plot represent the area of interest and the ellipses represent the ground sensor footprints. The first map represents NDVI from the drought year 2018 and the rest of the maps are from year considered with no drought
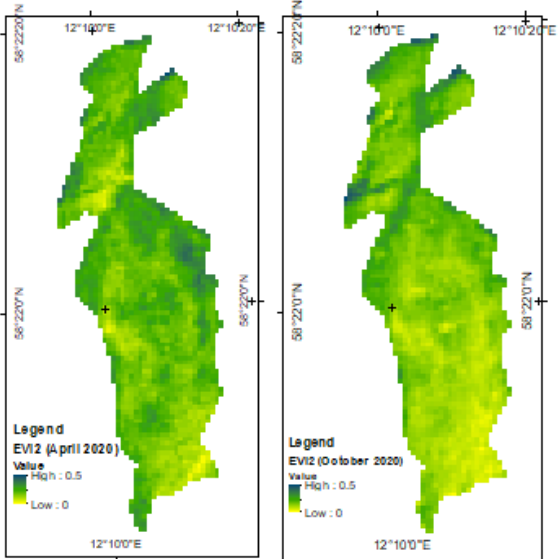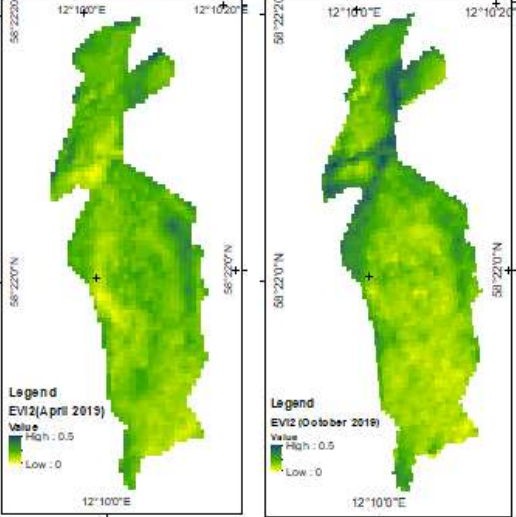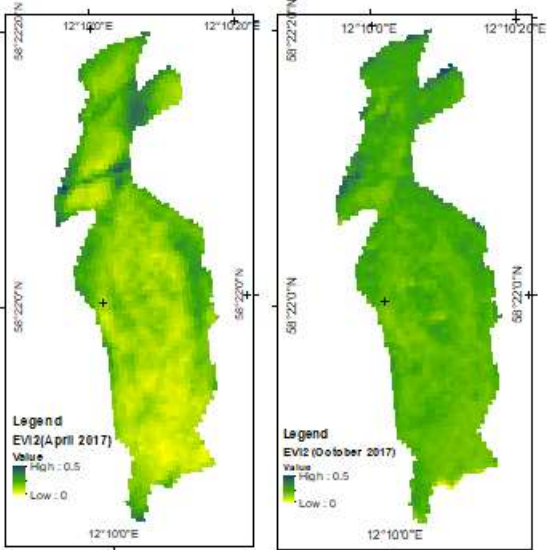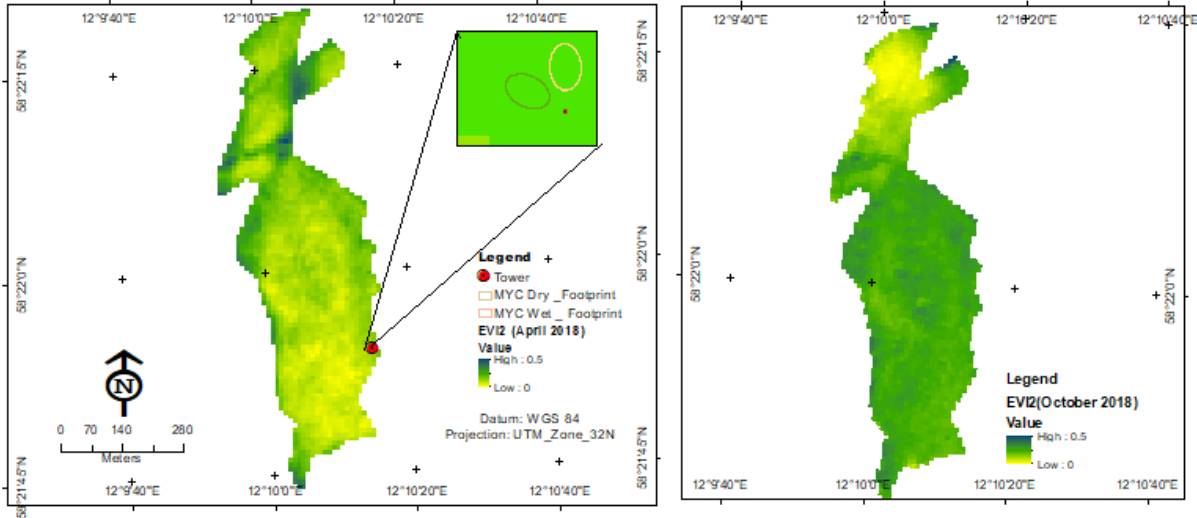
Figure 8: An example of EVI2 maps for the year in start of the season (April) and end of the season (October) from 2017 to 2020. The first map represents the EVI2 of the drought year 2018 and the rest of the maps are from year considered with no drought

4.3.2. Regression analysis

The comparison between VIs from Sentinel-2 and ground sensor were done using Pearson's correlation coefficient. Also, made correlation between the VIs from ground sensor data and VIs derived from Sentinel 2 versus the meteorological variables, to identify if meteorological data affect the mire productivity. The calculation of RMSE and correlation coefficients included identical date and time. The Sentinel-2 satellite overflies Skogaryd around 10h 40 min, therefore, the ground sensor VIs were selected in the same date and time of Sentinel-2 for comparison, while when comparing VIs from ground sensor against meteorological variables, it included the complete annual time series data.

To be able to know which meteorological variable affected the mire productivity during the drought episodes were divided in two episodes, one the 2018 (The drought year) and 2017, 2019, 2020 (the years considered with non-drought).

The goodness of fit of the model was evaluated based on the coefficient of determination (R^2) with standard measure values of range from 0 to 1, where the best model was determined by the highest R^2. The R^2 also shows the percentage of variability explained by the model (Peters, 2007).

Here was working with temporal data, but since was taking data from summer time, but not continuous data, there should not be autocorrelation. In addition, the hypothesis is that the data changes along the time, and that change is not related to time, but to other factors such as climate factors.

5. Results

5.1. Descriptive overview of meteorological data

First, a visual exploration of meteorological data (air temperature and relative humidity and precipitation) from 2017- 2020 were presented in figure 9. The precipitation was observed significantly lower in 2017 and 2018, compared to 2019 and 2020 (figure 9 c). The accumulated precipitation for year 2017 was 557.2 mm, of which, 143.0 mm fell in the summer. For 2018, the accumulated precipitation reached 705.0 mm, of which 124.6 mm fell in the summer if compared with 2019 and 2020 that is approximately a 39.6 % less rainfall than in regular years (Table 4).

The air temperature reached a mean of 20 ºC in summer 2018, being one of the warmest years in the study area. For the rest of observed years, the average maximum temperature reached the 16.5 ±1.3 ºC in summer (figure 9 b).

Year 2017 presented a high relative humidity (averaged RH: 80.85%), while 2018 was a relative dry year, especially in the summer (averaged RH for summer months: 64.85%). Years 2019 and 2020 presented milder relative humidity values (yearly accumulated RH: 78.23% and 75.28% for 2019 and 2020, respectively) (Table 4).

Considering these three meteorological variables together, 2018 was a year that can be considered into "drought" because the temperatures were ~5 ºC higher than for other years, but also the summer precipitations (124.6 mm) and relative humidity (64.8%) were lower in average than for other years. Precipitation was also lower in 2017 (figure 10 a), but the temperature was as other years and the RH higher, therefore P and RH mitigated the drought effects.
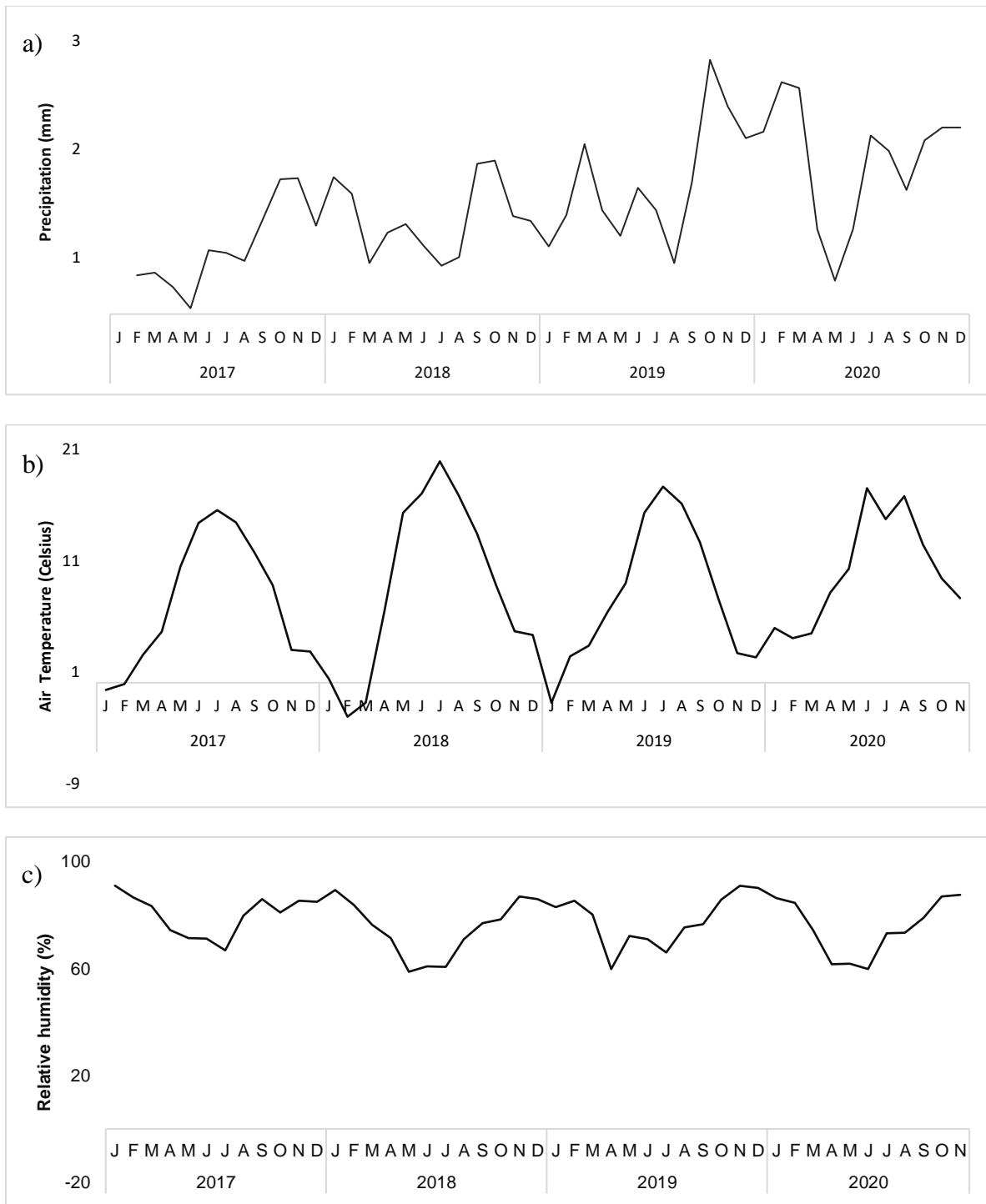
Figure 9: Plot of time series of monthly averaged meteorological variables. Air temperature, b), Relative humidity c) and precipitation a) from 2017 to 2020. The raw data in Mycklemossen is collected every 30 min, continuously.

Table 4: Accumulated precipitation and averaged relative humidity from years 2017 to 2020 and during the summer of the same period.

	Accumulated P, year (mm)	Accumulated P, summer (mm)	Averaged RH, year (%)	Averaged RH, summer (%)
2017	557.2	143.0	80.8	76.8
2018	705.0	124.6	75.4	64.5
2019	1083.4	232.6	78.5	75.2
2020	1009.8	272.4	75.2	59.6

*Values for 2020 are not for full year. The dataset ends in June 1st 2020.

5.2. Mires productivity observed by ground sensor VIs

VIs are a measure of plant productivity. The ground sensors located in Mycklemossen aim to monitor the productivity of mires along the time (figure 10). The dry mire showed higher productivity than wet mires along the year, and especially in the summer. NDVI values for the dry mire hit 0.9 in the summer and they reach these values earlier in the season around April (figure 10 a), while EVI2 values are up to 0.75 in the summer (figure 10 b).

The NDVI time series for the dry mire is stable for the observed years. The wet mire shows lower productivity than dry mire along the year, and especially in the summer. NDVI values for the wet mire hit 0.6 while EVI2 values are up to 0.5 in the summer.

We observe differences between NDVI and EVI2 for both the dry and wet mire in different years. NDVI looks stable for the dry mire along the observed time series (2017-2020); however, EVI2 is higher for 2017-2018 than in 2019-2020. In summer, we observe EVI2 reaches 0.75 in 2017, and the values go sequentially down in the next years: 0.65 in 2018, 0.55 in 2019 and 0.4 in 2020 (maximum values).

For the wet mire, the NDVI values are higher for 2018 (NDVI max = 0.57) and 2019, with a particular peak in the final part of 2019, which reaches 0.75. When compared with NDVI max for 2017 and 2020 (approx. 0.45), there was an increase in productivity of a 20%. A similar pattern is observed for EVI2; the EVI2max goes to 0.2-0.3 in 2017 and 2020, while it reaches 0.35 in 2018 and a similar highest peak in summer 2019, of 0.52.
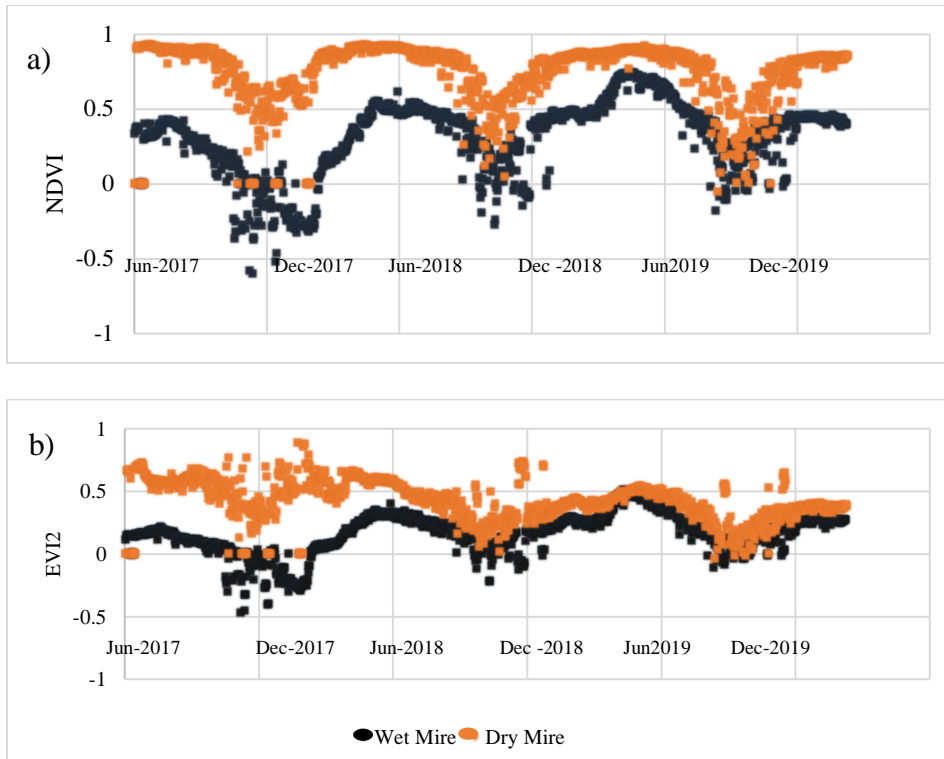
Figure 10: Time series of ground sensor based VIs namely EVI2 and NDVI from wet and dry mires, for June 2017 to May 2020. They are daily data from 9 AM to 2 PM with time resolution of 10minutes.

5.2.1.   VIs from Ground sensor correlation with Meteorological data

On summer 2018, when temperature increased, decrease of NDVI in wet mire, while in the dry mire the NDVI did not change with this temperature rise. The EVI2 in the wet mire; the productivity is higher when the temperatures are lower. The EVI2 in dry mire does not show clear correlation with TA (figure 11). During the summer, RH did not change significantly along the studied period (2017-2020). However, NDVI and EVI2 change along the time, for both dry and wet mire (figure 11). Therefore, at first sight, it is likely that RH is not a factor that influenced the mires productivity, alone. Only a correlation analysis could tell. The (figure9 c) shows that the precipitation does not influence the NDVI in wet mire and dry mire. The same happens for EVI2 for dry and wet mire. The accumulated precipitation could tell us the relationship the daily averaged precipitation.
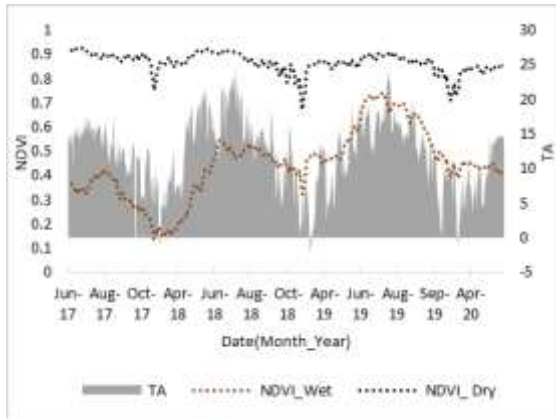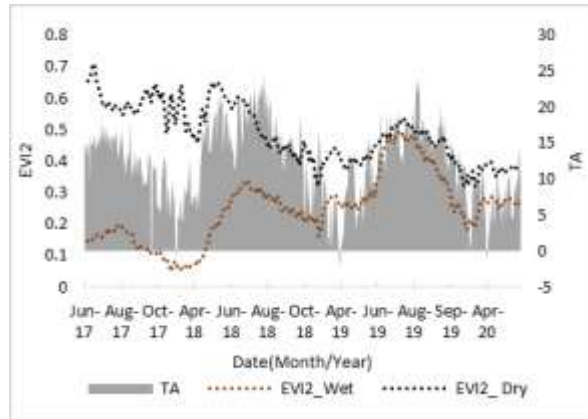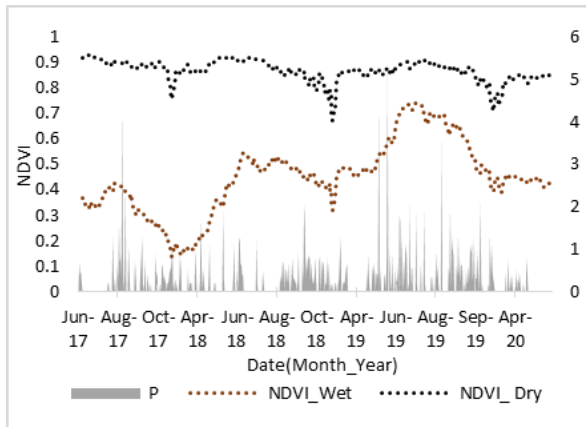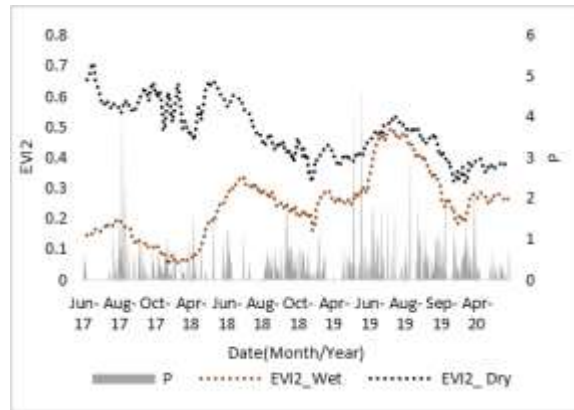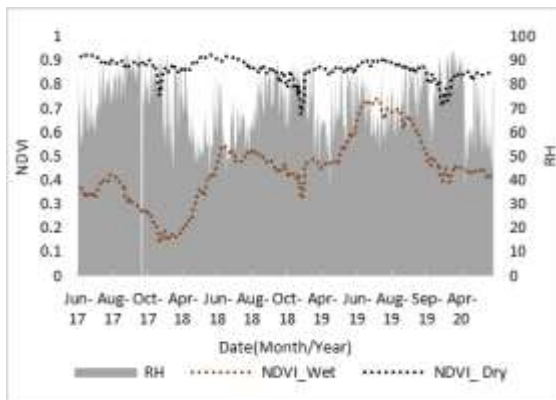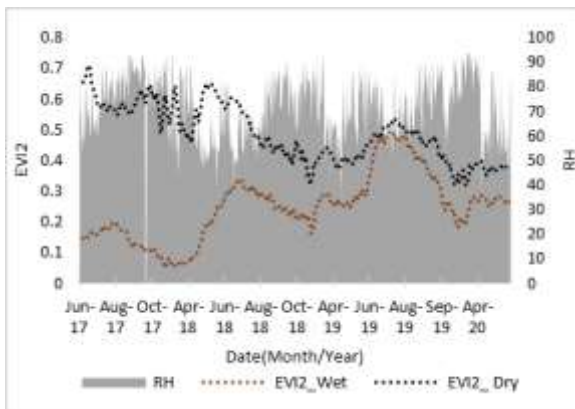
Figure 11: The plot of meteorological variables against vegetation indices from ground sensor in dry and wet mire. TA against NDVI a), TA against EVI2 b), P against NDVI c), P against EVI2 d), RH Vs NDVI e) and RH against EVI2 f), from 2017 (June-October), 2018 and 2019 (April-October)and 2020 (April-May).

5.2.1.1. Regression Analyses between NDVI and EVI2 derived by ground sensor data and meteorological data

First was explored the meteorological variables (TA, P and RH) to know if they affected the productivity of mire in Mycklemossen, measured through remote sensing VIs from ground sensor data. As shown in the results, TA and RH is more significant meteorological (P-value <0.0001 Table 5) in summer 2018 even in normal years (2017, 2019 and 2020) in both wet and dry mire. While the P is variable not significant in normal years and in drought year. In the drought year, the meteorological variable affected the mire productivity in ($R^2 \approx 40\%$) while in normal years, affected in ($R^2 \approx 26\%$). The R^2 is small not reaching 50% but the coefficient of determination in drought year is higher than normal year, meaning that RH and T affected mire productivity, but there are other variables that affected mire productivity on drought year that were not taken in to consideration.

Table5: Coefficients of determination and significance for the regression analyses between meteorological variables and ground sensor VIs in the 2018 considered as drought year and 2017,2019 and 2020 considered normal years

Year	Mire	Meteorological Variables	Ground Sensor NDVI			Ground Sensor EVI2		
			Coefficients of determination (R^2)	P-Value	RMSE	Coefficients of determination (R^2)	P-Value	RMSE
2018	dry	TA	0.369	0.000	0.051	0.347	0.000	0.077
		P		0.663			0.171	
		RH		0.000			0.000	
	wet	TA	0.381	0.000	0.099	0.418	0.000	0.068
		P		0.648			0.775	
		RH		0.000			0.083	
2017 2019 2020	dry	TA	0.266	0.000	0.0135	0.169	0.000	0.089
		P		0.000			0.014	
		RH		0.000			0.000	
	wet	TA	0.212	0.000	0.131	0.227	0.000	0.101
		P		0.03			0.135	
		RH		0.000			0.000	

5.2.2. VIs from Sentinel 2 correlation with Meteorological data

After generating VIs from Sentinel 2 and ground sensor, were filtered the values from both dataset to match spatially and temporally. Temporally selected the TA, RH and P records from ground sensor in the date and time of acquisition of Sentinel 2 images (Table 6).

Considering the three meteorological variables together the 2018 summer in both dry and wet mire the VIs decreased if compared with 2017, 2019 and 2020 and was the driest and warmest summer with average of RH = 37.7± 7.8 and TA = 21.9± 9.11 respectively.

Table 6: The averaged VIs from sentinel 2 and Meteorological variables in summer 2017-2020

Time	Sentinel -2				Meteorological data		
	NDVI-dry	NDVI-wet	EVI2-dry	EVI2-wet	TA (^{0}C)	RH (%)	P (mm)
2017	0.71± 0.05	0.54± 0.01	0.32± 0.01	0.25± 0.01	15.1± 5.7	68± 19.3	0,262 ± 0,17
2018	0.60± 0.03	0.53± 0.03	0.28± 0.05	0.33± 0.04	21.9± 9.11	37.7± 7.8	0,264 ± 0,14
2019	0.72± 0.05	0.70± 0.02	0.25± 0.01	0.41± 0.01	20.7± 5.6	63.1±19.6	0,431 ± 0,08
2020*	0.53± 0.04	0.61± 0.09	0.28± 0.04	0.36± 0.04	7.61± 3.4	75.6± 18.1	0,172 ± 0,05

4.2.2.1. Regression analyses between meteorological variables and Sentinel 2 VIs

First was explored the meteorological variables (TA, RH and P) to know how they affected the productivity of mires in Mycklemossen, measured through Sentinel 2 VIs. Based on the results; in general there is low and not significant correlation between Sentinel 2 and meteorological variables (Table 7).

Table 7: Coefficients of determination for the regression analyses between meteorological variables and Sentinel 2 VIs in the 2018 considered as drought year and 2017,2019 and 2020 considered normal years

Year	Meteorological variables	Mire	Sentinel 2_NDVI			Sentinel 2_EVI2		
			Coefficients of determination (R^2)	P-Value	RMSE	Coefficients of determination (R^2)	P-Value	RMSE
2018	TA	dry	0.163	0.524	0.016	0.105	0.561	0.077
	RH			0.848			0.767	
	P			0.629			0.811	
	TA	wet	0.296	0.721	0.030	0.208	0.967	0.068
	RH			0.912			0.821	
	P			0.846			0.853	
2017	TA	dry	0.136	0.588	0.082	0.136	0.202	0.039
	RH			0.476			0.244	
	P			0.105			0.117	
2019 2020	TA	wet	0.167	0.049	0.062	0.174	0.312	0.130
	RH			0.452			0.246	
	P			0.644			0.255	

5.2.3. Comparison of VIs derived from ground sensor data and Sentinel 2

The data collected includes April to October 2017, 2018 and 2019 April to October and April to May 2020. At first sight, there is a good agreement between the Sentinel 2 and ground sensor VIs, in terms of seasonal phenology. For NDVI of the wet mire, the Sentinel 2 observations fall very close to the ground data measures. For the rest of cases (NDVI – dry mire and EVI2), Sentinel 2 data follow the trend (figure 12), but there is an offset with the ground sensor data. In the case of NDVI – dry mire, the Sentinel 2 values are lower than for the ground sensors with average of ground sensor NDVI 0.86± 0.02 and Sentinel-2 NDVI 0.61± 0.04). For EVI2, in wet mire the Sentinel 2 values are higher than for ground sensors with average of EVI2 Sentinel-2 (0.35 ± 0.03) and ground sensor (0.25 ± 0.02) (Table 8).

Table 8: VIs values during the growing season for Sentinel 2 and ground sensors in Mycklemossen during 2017 to 2020 in wet and dry mire ecosystem

		Ground sensor		Sentinel 2	
		NDVI	EVI2	NDVI	EVI2
Dry mire	2017	0.89± 0.019	0.59± 0.05	0.68± 0.012	0.33± 0.014
	2018	0.88± 0.02	0.54± 0.05	0.59± 0.052	0.28± 0.029
	2019	0.86± 0.02	0.45± 0.05	0.65± 0.082	0.24± 0.025
	2020	0.83± 0.02	0.37± 0.05	0.59± 0.007	0.29± 0.012
	TOTAL	0.86± 0.02	0.48± 0.2	0.61± 0.165	0.28± 0.02
Wet mire	2017	0.35± 0.03	0.15± 0.02	0.54± 0.051	0.24± 0.010
	2018	0.41 ± 0.05	0.23± 0.03	0.52± 0.035	0.33± 0.053
	2019	0.59± 0.05	0.35± 0.03	0.69± 0.021	0.40± 0.024
	2020	0.43± 0.05	0.26± 0.02	0.54± 0.014	0.42± 0.016
	TOTAL	0.44± 0.18	0.25± 0.02	0.57± 0.12	0.35± 0.03
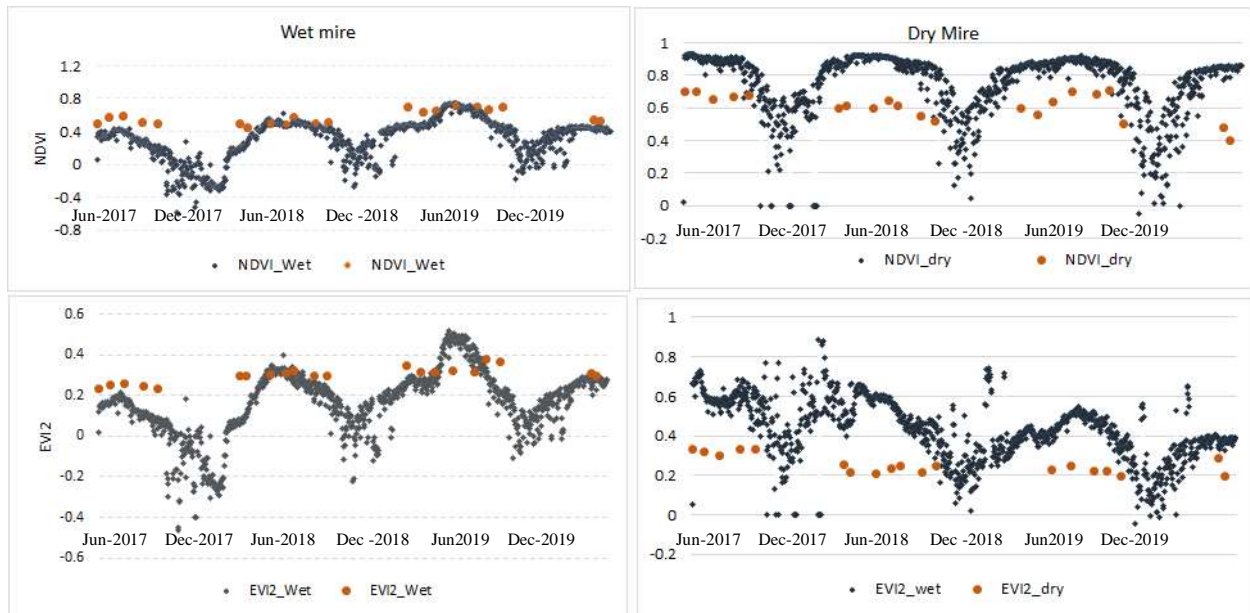
Figure 12: NDVI and EVI2 from ground sensor data, daily averaged (9 am to 2 pm) overlapped with Sentinel 2 data for June to October in 2017, April to October in 2018- 2019 and April –May in 2020, in both dry and wet mire ecosystem (in the left).

5.2.3.1.Regression analyses between ground sensor and Sentinel 2 VIs

At a glance, there is a relationship between VIs (NDVI and EVI2) from Sentinel 2 and VIs from ground sensor and reflected by a positive correlation As the VIs from Sentinel 2 increases, VIs from ground sensor also tends to increase however, it is not a perfect relationship.

Pearson's correlation takes all of the data points on the graph and represents them as a single number. In this case, the statistical output indicates that the Pearson's correlation coefficient ($r^2 >$ 0.5, Table 9).

The highest correlation was observed between ground sensor and Sentinel 2 EVI2, for the wet mire, although all values present similar coefficients of determination and the P-value (< 0.0001) shows significant relationship between ground sensor and Sentinel 2VIs.

Table 9: The Coefficients of determination for the regression analyses between ground sensor and Sentinel 2 VIs from 2018-2020.

	Sentinel 2 NDVI vs. Ground sensor NDVI			Sentinel 2 EVI2 vs. Ground sensor EVI2		
	Determination coefficient (R^2)	P-value	RMSE	Determination coefficient (R^2)	P-value	RMSE
Dry	0.592	< 0.0001	0.02	0.504	< 0.0001	0.03
Wet	0.509	< 0.0001	0.06	0.635	< 0.0001	0.04

This is good agreement with what the visual assessment reflected in (Figure 12). In figure 12 a) represents plot of NDVI from ground sensor and NDVI from Sentinel 2 in wet mire. The Sentinel 2 NDVI coefficient in the regression equation is 1.0624. This coefficient represents the mean increase of NDVI of ground sensor for every additional Sentinel 2 NDVI. If your Sentinel 2 NDVI increases by 1for example, the average of NDVI from ground increases by 1.0624. In figure 12 b) represents plot of NDVI from ground and Sentinel 2 in dry mire. The Sentinel 2 NDVI coefficient in the regression equation is 0.2591. In the figure, 13 c) represents plot of EVI2 from ground and Sentinel 2 in wet mire.

The Sentinel 2 EVI2 in wet mire coefficient in the regression equation is 0.4267 and in Figure 12 d) represents plot of EVI2 from ground and Sentinel 2 in dry mire. The Sentinel 2 EVI2 in dry mire coefficient in the regression equation is 0.6309.
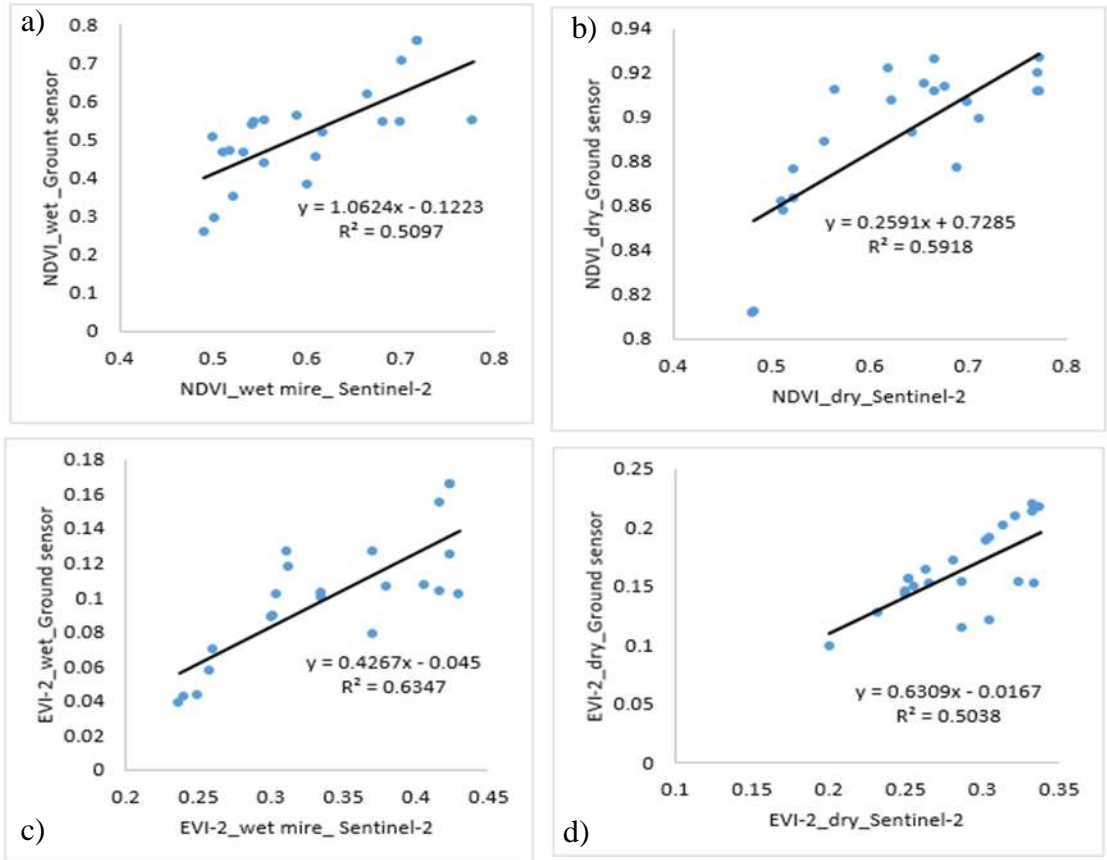
Figure 123: Plot of the ground sensor VIs against the Sentinel 2 VIs both a), b), c) and d) with positive correlation, with (p-value < 0.0001)

6. Discussion

6.1. Are the NDVI and EVI2 derived by satellite images and ground sensor data correlated with meteorological data?

In this research, an aim has been made to use time series of meteorological data and remote sensing data (Sentinel 2 and ground sensor data) to observe if the drought in 2018 compromised the productivity of mires in Skogaryd.

Based on remote sensing, was monitored the productivity of vegetation and possible effects of the drought in 2018, with the help of VIs such as NDVI and EVI2.

The NDVI has generally higher values than EVI2, and showed larger differences between the normal years and drought year. This could be because NDVI reach high values and has a steeper increase in values than EVI2 as a response change in vegetation (Jiang et al., 2008). The EVI2 was more suitable for measuring differences in vegetation productivity in regions with high biomass, where NDVI has often reached its maximum value (Jiang et al., 2008). The NDVI tend to saturate at regions high biomass values (Reed et al. 2009; Huete et al. 2002) As could be seen on figure 9, NDVI in dry mire saturates during the growing season. In this research, NDVI was used because it is the most frequent VI used, but as it is prone to saturation and noise caused by the color of the soil and water, it was interesting to use EVI2, a less prone VI to these problems (Villa et al. 2014).

The 10 m resolution data from Sentinel-2 satellite can stress in vegetation stress, but has limitations to quantify productivity in dry mires. This is probably due to the saturation of VIs when the productivity of dry mires increase.

As the mire ecosystems are characterized by a high degree of spatiotemporal complexity because their combined spatial heterogeneity with seasonal dynamics (Reschke and Hüttich 2014). The heterogeneous ecosystems there are rapid changes in the NDVI signal in which may bias such estimators.

Based on meteorological data (TA and RH) in summer 2018 was unusually warm and dry, compared with summer of 2017, 2019 and 2020. It is also remarkable that 2019 was a year with a unusual high precipitation, which could have helped to the resilience of mires in the long term.

This research explored which meteorological variable (TA, RH or P) affects more significantly to mire productivity. For this, was performed regression analyses between remote sensing VIs and meteorological data. The mean monthly air temperature during the growing season of 2018 was higher than 2017, 2019 and 2020. The results showed that the AT was the main meteorological factor that affected NDVI and EVI2 changes in Skogaryd's dry and wet mire, which founding was consistent with that results in the publication literature by (Zhao, 2004). According to our results TA and RH affect more the wet mire than the dry mire. We did not observe any significant correlation between precipitation and productivity.

The VIs showed more clearly the effects of drought in wet mire ecosystem than dry mire. The impact of the 2018 drought on vegetation was clear in April, at the beginning of the season, when VIs values were generally lower in 2018 than 2017, 2019 and 2020. This drop in VIs values in June is indicative of the effect of drought on vegetation that manifests itself through reduced photosynthetic activity (Jones & Vaughan, 2010) and reduced amount of water in the vegetation (Gao, 1996). Therefore, the drought retarded the start of the growing season in the studied wet mire. The highest value of VIs during a growing season in southern Sweden is expected to be in June (Walker et al, 2011). Another significant finding of our study is that NDVI and EVI2 calculated from ground sensors showed different productivity values in the observed period. The productivity of the wet mire was lower during warm summers according to NDVI, but no big change was reported for dry mire. In the case of EVI2, the dry mire showed higher productivity in hot summers, while wet mire's productivity was low.

6.2. Are NDVI and EVI2 from Sentinel-2 correlated with the similar VIs from ground sensor data?

When comparing Sentinel 2 VIs against ground sensor VIs, both data types follow the same trend along the time.

EVI2 make use of the same spectral bands as NDVI (red and NIR) and was developed to overcome a series of weaknesses that NDVI shows, such as saturation in abundant vegetation (large area index) and sensitivity to atmospheric effect and soil brightness (Gitelson, 2004). In our case, a mire, leaf area index is not a limitation. However, in Northern latitudes and because the light colors of mire vegetation, NDVI can be subjected to light scattering and illumination problems.

In addition, there are some noticeable differences between the indices. First, the EVI2 response is less intense than NDVI during the growing season. Probably, the reason for not observing changes in NDVI in dry mire is due to the NDVI becoming saturated as the vegetation becomes lush in a warm summer. If compared with EVI2, the dry mire increases productivity in the warmer years. Our results partially agree with previous research (Reinermann et al. 2019), which showed that VIs values are generally lower in dry summers compared to a normal summer. In our case, this statement is only true for the wet mire.

The correlation between VIs from Sentinel-2 and ground sensors showed a mild positive significant correlation. The mild correlation might be explained by the fact that Sentinel 2 represents well the productivity trend along the time, but there is certain bias between satellite and ground data. In the case of the dry mire, the offset is around a 25% less in Sentinel 2 than groun sensor. This is again a sign that the dry mire color and brightness saturates VIs and is affected by atmospheric scattering (Pan, 2018). In addition, the difference in data frequency between Sentinel 2 and ground data might be a factor for the low correlation between dataset.

6.3. Is dry mire more drought-resistant than wet mire?

For our observed scenario, dry mire vegetation has a remarkable capacity to adapt to climate variability, even increasing productivity in warm and dry years. Dry wetlands are resilient ecosystems because can adapt to extreme periodic drought–flood episodes and to climate change (Leigh, 2010). During droughts, the dry mire show resilience to water availability due to drought-tolerant plant species (Capon, 2003). Dry mires can tolerate many years without water and can regenerate quickly after floods, while wet mire vegetation reduces its extent during droughts, but responds immediately for seed re-wetting or rhizome regeneration (Capon, 2016). This resilience of wet mire depends on periodic flooding (Leigh, 2010). This can be explained by the ground water reserves and soil humidity of the mires, which makes them resilient ecosystems.

In this study, the wet mire was affected negatively to the drought and warm weather in 2017 and 2018, but recovered nicely in 2019 and 2020, probably because of the high precipitation in 2019. Some effects of vegetation deterioration due to drought are less obvious, for example, interruptions in primary sources in the food chain due to loss of vegetation in wetlands (Maestre, 2012). The

changes in climate generated a decrease in uptake of water in summer 2018 (124.6 mm) comparing to 2019 and 2020, which aggravated the impacts of the drought.

The results presented here provide quantifiable projections of deterioration of wet mire and resistance of dry mire in climate change.

6.4.   Limitations

In this study, the data acquisition time was very important. There are some limitations with Sentinel-2 data availability. Therefore, having more images for each year or more similar dates would have given better comparison about differences in productivity between these years.

The Sentinel 2 data used was sometimes affected by different aerosol conditions, which could slightly affect the reflectance of the observed mires and therefore the VIs values.

A third consideration is that the three-used dataset (satellite, multispectral ground sensors and meteorological data) comprehend significant differences in spatial and temporal resolution. Therefore, even though selecting similar periods and area, there can be differences in the time and space aggregation.

The utilized Sentinel-2 images have a resolution of 10 meters, and each pixel of Sentinel-2 100m^2. The ground sensors produced two footprint that cover a small area (23.6 m^2), close to each other. To compare Sentinel 2 and ground sensors, was selected the proportion of the pixels that cover the ground sensor footprints. However, the Sentinel 2 pixels present reflectance mixing of different targets than the ground sensors actually see.

6.5.   Recommendations

Future patterns of global climate change and projections of inter-country variability indicate that droughts will be longer in rain-fed areas due to possible changes in weather patterns, what could lead to the global decreases in the extent of wetlands, deterioration of vegetation and decreases in habitat services. Although these are recognized risk of pronounced inter-country variability and climate change, vegetation deterioration estimates in arid wetland areas are still uncertain, often

due to the simplified representation of flood and drought episodes and the response of vegetation to these events (Tooth, 2018; Power et al. 2013).

The 2018 drought was shown to have a marked impact on the vegetation in the study area. To better predict and prepare for future drought events, more research in the area would be beneficial. Future studies could gain from using more images for each year to better capture changes over the season.

7.   Summary and conclusions

The aim of the study was to use satellite remote sensing and ground sensors as a method to investigate whether the drought during the summer of 2018 affected mires in southern Sweden.

The summer 2018 was unusually warm (16.3 $^{\circ}$C), Averaged and dry 64.5%, compared with summer of 2017, 2019 and 2020. It is also remarkable that 2019 was a year with an unusual high precipitation (1083.4 mm), which could have helped to the resilience of mires in the long term.

The results of this study showed that EVI2 is a better indicator of the effect of drought on vegetation than NDVI, since the latter saturates at higher mire productivity and in satellite data, due to atmospheric interference.

The TA and RH are the meteorological variables that affected mire productivity in Skogaryd. These two meteorological variables are more important during drought events. TA and RH were the main meteorological factors that affected mire productivity changes in Skogaryd, as observed by ground sensors and affected more the wet mire than the dry mire, as observed by ground sensors. Was not observed any significant correlation between precipitation and productivity. There was no correlation between meteorological data and Sentinel 2 VIs.

The correlation between VIs from Sentinel-2 and ground sensors showed a positive significant correlation. For the observed scenario, dry mire vegetation has a remarkable capacity to adapt to climate variability, even increasing productivity in warm and dry years.

8.   References

Ågren, A., M. Berggren, M. Jansson, and H. Laudon (2008), Terrestrial export of highly bioavailable carbon from small boreal catchments during spring flood, Freshw. Biol., doi:10.1111/j.1365-2427.2008.01955.x.

Allan Buras, Anja Rammig, Christian S. Zang (2019). "Quantifying impacts of the   2018 drought on European ecosystems in comparison to 2003".

Allen, C.D.; Macalady, A.K.; Chenchouni, H.; Bachelet, D.; McDowell, N.; Vennetier, M.; Kitzberger, T.; Rigling, A.; Breshears, D.D.; Hogg, E.T (2010). "A global overview of drought and heat-induced tree mortality reveals emerging climate change risks for forests". For Ecol. Manag. 259, 660–684.

Anjum, S. A., Ashraf, U., Tanveer, M., Khan, I., Hussain, S., Shahzad, B., et al. (2017). Drought induced changes in growth, osmolyte accumulation and antioxidant metabolism of three maize hybrids. Front. Plant Sci. 8:69. doi: 10.3389/fpls.2017.0006

AghaKouchak, A., A. Farahmand, F. S. Melton, J. Teixeira, M. C. Anderson, B. D. Wardlow, and C. R. Hain. (2015). Remote sensing of drought: "Progress, challenges and opportunities. Reviews of Geophysics", 53: 452-480. DOI: 10.1002/2014rg000456.

Banzhaf, Stefan & Klemedtsson, Leif & Sturkell, Erik & Nyström, Elin & Barthel, Roland. (2015). Hydrogeological and geophysical investigations to evaluate groundwater influences on GHG emissions at the national research site Skogaryd.

Bennett Bennett, A.C.; McDowell, N.G.; Allen, C.D.; Anderson-Teixeira, K.J. (2015). "Larger trees suffer most during drought in forests worldwide". Nat. Plants, 1, 15139.

Bubier J, Moore T, Savage K, Crill P. (2005). "A comparison of methane flux in a boreal landscape between a dry and a wet year. Global Biogeochem". Cycles 19, 11. (doi:10.1029/2004gb002351)

Carlson, Toby & Ripley, David. (1997). On the Relation between NDVI, Fractional Vegetation Cover, and Leaf Area Index. Remote Sensing of Environment. 62. 241-252. 10.1016/S0034-4257(97)00104-1.

Capon, S. J. & Reid, M. A. (2016). Vegetation resilience to mega-drought along a typical floodplain gradient of the southern Murray–Darling Basin, Australia. J. Veg. Sci. 27, 926–937.

Capon, S. J. (2003). Plant community responses to wetting and drying in a large arid floodplain. River Res. Appl. 19, 509–520.

Cashion, J., V. Lakshmi, D. Bosch, and T. J. Jackson (2005). Microwave remote sensing of soil moisture: Evaluation of the TRMM microwave imager (TMI) satellite for the Little River Watershed Tifton, Georgia, J. Hydrol., 307(1), 242–253, doi:10.1016/j.jhydrol.2004.10.019.

Cherenkova, Elena & Kononova, Nina & Muratova, Nadiya. (2013). Summer Drought 2010 In The European Russia. Geography, Environment, Sustainability. 6. 10.15356/2071-9388_01v06_2013_04.

Ciais, P.; Reichstein, M.; Viovy, N.; Granier, A.; Ogée, J.; Allard, V.; Aubinet, M.; Buchmann, N.; Bernhofer, C.; Carrara, A.; et al.(2005). Europe-wide reduction in primary productivity caused by the heat and drought in 2003. Nature 2005, 437, 529–533.

D.P. Roy M.A. Wulder (2014). "Landsat-8: Science and product vision for terrestrial global change research". Remote Sensing of Environment 145 (2014) 154–172of Applied Earth Observation and Geoinformation, Vol. 30.

Davidson, Eric & Janssens, Ivan. (2006). Temperature Sensitivity of Soil Carbon Decomposition and Feedbacks to Climate Change. Nature. 440. 165-73. 10.1038/nature04514.

Dotzler, Sandra & Hill, Joachim & Buddenbaum, Henning & Stoffels, Johannes. (2015). The Potential of EnMAP and Sentinel-2 Data for Detecting Drought Stress Phenomena in Deciduous Forest Communities. Remote Sensing. 7. 14227-14258. 10.3390/rs71014227.

Drusch, M. & 14 co-authors (2012). Sentinel-2: ESA's optical high-resolution mission for GMES operational services, Rem. Sens. Env. (accepted).

Entekhabi, D., et al. (2004), The hydrosphere state (Hydros) satellite mission: An Earth system pathfinder for global mapping of soil moisture and land freeze/thaw, IEEE Trans. Geosci. Remote Sens., 42(10), 2184–2195, doi:10.1109/TGRS.2004.834631.

European Environment Agency (2020). INDICATOR ASSESSMENT- Vegetation productivity. In link: https://www.eea.europa.eu/data-and-maps/indicators/land-productivity-dynamics/assessment

European Spatial Agency (2020). Sen2cor. Retrieved October 12, 2020, from http://step.esa.int/main/snap-supported-plugins/sen2cor/

European Spatial Agency (2017). Sentinel-2 L2A products available on Sentinel Hub. In link: https://medium.com/sentinel-hub/sentinel-2-l2a-products-available-on-sentinel-hub-beab58903285

Farooq, M., Wahid, A., Kobayashi, N., Fujita, D., and Basra, S. M. A. (2009b). Plant drought stress: effects, mechanisms and management. Agron. Sustain. Dev. 29, 185–212. doi: 10.1051/agro:2008021.

Flink, Erica, and Ville Stålnacke. (2019). "Torkan 2018 Och Dess Påverkan På Skogsvegetation Skogaryd Och Västra Tunhem , Västra Götaland."

Gao, (1996)"NDWI—A normalized difference water index for remote sensing of vegetation liquid water from space.

Galambosi, Bertalan & Takkunen, N. & Repcák, M.. (2000). The effect of regular collection of Drosera rotundifolia in natural peatlands in Finland: Plant density, yield and regeneration. Suo. 51. 37-46.

Gitelson, A A. (2004) "Wide Dynamic Range Vegetation Index for Remote Quantification of Biophysical Characteristics of Vegetation." Journal of Plant Physiology, 161: 165–173.

Gu Y, Brown JF, Verdin JP, Wardlow B (2007). A five-year analysis of MODIS NDVI and NDWI for grassland drought assessment over the central Great Plains of the United States. Geophys Res Lett 34:L06407.

Grip H. and Rodhe A., 1994: Vattnets väg från regn till bäck. 3:rd revised issue. Hallgren & Fallgren Studieförlag AB. Karlshamn. Sweden

Heimann, Martin & Reichstein, Markus. (2008). Heimann M, Reichstein M.. Terrestrial ecosystem carbon dynamics and climate feedbacks. Nature 451: 289-292. Nature. 451. 289-92. 10.1038/nature06591.

Hänninen, Heikki & Tanino, Karen. (2011). Tree seasonality in a warming climate. Trends in plant science. 16. 412-6. 10.1016/j.tplants.2011.05.001.

Hu, Shu Ping. (2010) Simple Mean, Weighted Mean, or Geometric Mean. ISPA/SCEA Professional Development and Training Workshop San Diego, CA.

Huete, A., Didan, K., Miura, T., Rodriguez, E. P., Gao, X., & Ferreira, L. G. (2002). Overview of the radiometric and biophysical performance of the MODIS vegetation indices. Remote Sensing of Environment, 83(1-2), 195-213. https://doi.org/10.1016/S0034-4257(02)00096-2

IPCC,"Climate change (2007): the physical science basis,"inContribution of WorkingGroup I to the Fourth Assessment. Report of the Intergovernmental Panel on ClimateChange, S. Solomon et al., Eds., Cambridge University Press, Cambridge, United Kingdom/New York, pp. 996

Jackson RD, Huete AR (1991) Interpreting vegetation indexes. Prev Vet Med 11:185–200

Jiang et al., 2008 Z. Jiang, A.R. Huete, K. Didan, T. Miura Development of a two-band enhanced vegetation index without a blue band Remote Sensing of Environment, 112 (2008), pp. 3833-3845

Jones, H., & Vaughan, R. (2010). Remote sensing of vegetation : Principles, techniques, and applications. Oxford; New York: Oxford University Press.

Kelman, I.; Gaillard, J.; Lewis, J.; Mercer, J. (2016). "Learning from the history of disaster vulnerability and resilience research and practice for climate change". Nat. Hazards, 82, 129–143.

L. Klemedtsson, M. Ernfors, R.G. Björk, P. Weslien, T. Rütting, P. Crill, U. (2010). Sikström Reduction of greenhouse gas emissions by wood ash application to a Picea abies (L.) Karst. forest on a drained organic soil, Eur. J. Soil Sci., 61 pp. 734-744.

Lappalainen, E. (ed.) 1996a. Global Peat Resources. International Peat Society and Geological Survey of Finland, Saarijärvi, Finland.

Leigh, C., Sheldon, F., Kingsford, R. T. & Arthington, A. H. (2010). Sequential floods drive booms and wetland persistence in dryland rivers: A synthesis. Mar. Freshw. Res. 61, 896–908.

Li, C., Jiang, D., Wollenweber, B., Li, Y., Dai, T., and Cao, W. (2011). Waterlogging pretreatment during vegetative growth improves tolerance to waterlogging after anthesis in wheat. *Plant Sci.* 180, 672–678. doi: 10.1016/j.plantsci.2011.01.009

Linderson, M.-L., J. Holst, M. Heliasz, L. Klemedtsson, A. Klosterhalfen, A. Krasnova, A. Läänelaid, H. Linderson, et al. (2020). "Boreal forest carbon exchange and growth recovery after the summer 2018 drought". EGU General Assembly 2020. DOI: 10.5194/egusphere-egu2020-10559

Mezbahuddin, Symon & Grant, R.F. & Hirano, Takashi. (2013). Modelling effects of seasonal variation in water table depth on net ecosystem CO2 exchange of a tropical peatland. Biogeosciences Discussions. 10. 13353-13398. 10.5194/bgd-10-13353-2013.

Maestre, F. T. et al. (2012). Plant species richness and ecosystem multifunctionality in global drylands. Science 335, 214–218).

Minayeva, Tatiana & Bragg, Olivia & Sirin, A.. (2017). Towards ecosystem-based restoration of peatland biodiversity. 19. 10.19189/MaP.2013.OMB.150.

Monteith, J.. (2006). A reinterpretation of stomatal response to humidity. Plant, Cell & Environment. 18. 357 - 364. 10.1111/j.1365-3040.1995.tb00371.x.

Myneni RB, Hall FG, Sellers PJ, Marshak AL (1995) The interpretation of spectral vegetation indexes. IEEE T Geosci Remote 33:481–486.

Påhlsson L (1998) Vegetationstyper i Norden, København, Nordisk Ministerråd.

Pan, Y.Y.; Li, C.C.; Ma, X.X.; Wang, B.S.; Fang, X. (2018,). Atmospheric correction method of sentinel-2A satellite and result analysis. Remote Sens. Inf. 33, 41–48.

Peters, A.J., Walter-Shea, E.A., Ji, L., Vina, A., Hayes, M., and Svoboda, M.D. (2002). Drought monitoring with NDVI-based standardized vegetation index. Photo-gramm. Eng. Rem. S.68(1): 71–75.

Persson, M., E. Lindberg & H. Reese (2018) Tree Species Classification with MultiTemporal Sentinel-2 Data. Remote Sensing, 10,

Puletti, N., F. Chianucci, and C. Castaldi. (2018).,"Use of Sentinel-2 for forest classification in Mediterranean environments,"Ann. Silvicultural Res.42(1), 32–38

Puletti, N., W. Mattioli, F. Bussotti, and M. Pollastrini. (2019). Monitoring the effects of extreme drought events on forest health by Sentinel-2 imagery. Journal of Applied Remote Sensing, 13. DOI: 10.1117/1.Jrs.13.020501

Power, S., Delage, F., Chung, C., Kociuba, G. & Keay, K. (2013). Robust twenty-first-century projections of El Niño and related precipitation variability. Nature 502, 541.

Reed, B.C.; Schuwartz, M.D.; Xiao, X. Remote sensing phenology: Status and the way forward. In Phenology of Ecosystems Processes; Springer: Berlin, Germany, 2009; pp. 231–246.

Reichstein, Markus & Ciais, Philippe & Papale, D.. (2007). "Reduction of ecosystem productivity and respiration during the European summer 2003 climate anomaly: a joint flux tower, remote sensing and modelling analysis". Global Change Biology. 12. 1-18.

Reinermann, Sophie & Gessner, Ursula & Asam, Sarah & Kuenzer, Claudia & Dech, Stefan. (2019). The Effect of Droughts on Vegetation Condition in Germany: An Analysis Based on Two Decades of Satellite Earth Observation Time Series and Crop Yield Statistics. Remote Sensing. 11. 1783. 10.3390/rs11151783.

Rennenberg, H.; Loreto, F.; Polle, A.; Brilli, F.; Fares, S.; Beniwal, R.S.; Gessler, A. (2006). Physiological responses of forest trees to heat and drought. Plant Biol, 8, 556–571.

Reschke, J., and C. Hüttich. 2014. "Continuous Field Mapping of Mediterranean Wetlands Using Sub-pixel Spectral Signatures and Multi-temporal Landsat Data." International Journal of Applied Earth Observation and Geoinformation 28: 220–229. doi:10.1016/j.jag.2013.12.014.

Richardson A, et al. (2013) Physical and genetic associations of the Irc20 ubiquitin ligase with Cdc48 and SUMO. PLoS One 8(10):e76424.

Rondeaux, G., M. Steven, and F. Baret. 1996. "Optimization of Soil-Adjusted Vegetation Indices." Remote Sensing of Environment 55: 95–107. doi:10.1016/0034–4257(95)00186–7.

Rosenzweig, Cynthia, Ana Iglesias, X. B. Yang, Paul R. Epstein, and Eric Chivian. (2001). "Implications for Food Production, Plant Diseases, and Pests." *Global Change and Human Health* 2(2):90–104.

Rouse J., Jr., R. Haas, J. Schell, and D. Deering,(1974). "Monitoring vegetation systems in the great plains with ERTS," NASA, Washington, DC, USA, vol. 351, pp. 309–317.

Rulinda, Coco & Dilo, Arta & Bijker, Wietske & Stein, Alfred. (2012). Characterising and quantifying vegetative drought in East Africa using fuzzy modelling and NDVI data. Journal of Arid Environments - J ARID ENVIRON. 78. 169-178. 10.1016/j.jaridenv.2011.11.016.

Rydin, Håkan & Sjörs, H. & Löfroth, M.. (1999). 7. Mires. Acta Phytogeographica Suecica. 84. 91-112.

Schlesinger, William & Andrews, Jeffrey. (2000). Soil Respiration and Global Carbon Cycle. Biogeochemistry. 48. 7-20. 10.1023/A:1006247623877.

Scurlock et al., (2001). J.M.O. Scurlock, G.P. Asner, S.T. Gower Worldwide Historical Estimates and Bibliography of Leaf Area Index, 1932–2000. ORNL Technical Memorandum TM-2001/268 Oak Ridge National Laboratory, Oak Ridge, TN.

Skogaryd Research Catchment. 2018. Meteorological data from Mycklemossen, 2017. SITES Data Portal. https://hdl.handle.net/11676.1/gFHqMeAdPbHjsxvYi7nLWHC0.

Skogaryd Research Catchment. 2018. Meteorological data from Mycklemossen, 2018-01-01–2018-12-31. SITES Data Portal. https://hdl.handle.net/11676.1/nlP1-wHXFPkO8VJXjxSbilvc.

Skogaryd Research Catchment. 2020. Reflectance and Spectral Vegetation Indices from Mycklemossen, 2017-06-23–2020-06-01. SITES Data Portal. https://hdl.handle.net/11676.1/zCl6fY2N0ozurQV7W_SrgzKl.

Skogaryd Research Catchment. 2020. Meteorological data from Mycklemossen, 2019. SITES Data Portal. https://hdl.handle.net/11676.1/CzQ1XRzyCqprClwU18i5vH2c.

Skogaryd Research Catchment. 2021. Meteorological data from Mycklemossen, 2020. SITES Data Portal. https://hdl.handle.net/11676.1/fJ9X7srjRsEOQC1v5yNY_3VE.

Sorooshian, S., et al. (2011), Advanced concepts on remote sensing of precipitation at multiple scales, Bull. Am. Meteorol. Soc., 92(10), 1353–1357.

Stephenson D. B. (2008),"Definition, diagnosis, and origin of extreme weather and climateevents,"inClimate Extremes and Society, H. F. Diaz and R. J. Murnane, Eds., CambridgeUniversity Press, Cambridge, pp. 11–23 .

Satellite Imaging Corporation (SIC). (2016). Sentinel-2A Satellite Sensor (10m). Retrieved August 7, 2016, from http://www.satimagingcorp.com/satellite-sensors/other-satellite-sensors/sentinel-2a/

SITES, (2018). Guidelines for multispectral data collection, Department of Physical Geography and Ecosystem Science.

Skye, (2020). Instrument for monitoring our environment, from: https://www.skyeinstruments.com/minimet/.

Tooth, S. (2018). The geomorphology of wetlands in drylands: Resilience, nonresilience, Geomorphology 305, 33–48.

Töyrä, Jessika & Pietroniro, Alain. (2005). Towards Operational Monitoring of a Northern Wetland Using Geomatics-Based Techniques. Remote Sensing of Environment. 97(2). 174-191. 10.1016/j.rse.2005.03.012.

Villa, P.; Mousivand, A.; Bresciani, M. Aquatic vegetation indices assessment through radiative transfer modeling and linear mixture simulation. Int. J. Appl. Earth Obs. Geoinf. 2014, 30, 113–127.

Vicente-Serrano SM. (2006). Spatial and temporal analysis of droughts in the Iberian Peninsula (1910–2000). Hydrol. Sci. J. 51(1): 83–97.

Walker, D.A.; Bhatt, U.S.; Callaghan, T.V.; Comiso, J.C.; Epstein, H.E.; Forbes, B.C.; Gill, M.; Gould, W.A.; Henry, G.H.R.; Jia, G.J.; Kokelj, S.V.; Lantz, T.C.; Oberbauer, S.F.; Pinzon, J.E.; Raynolds, M.K.; Shaver, G.R.; Tucker, C.J.; Tweedie, C.E.; Webber, P.J. (2011). Vegetation. Pages 89-95 i Richter-Menge, J.; Jeffries, M.O.; Overland, J.E., eds. Arctic Report Card.

Wilhite, D.A. (2000). Drought as a natural hazard: Concepts and definitions. In Drought: A Global Assessment; Routledge: New York, NY, USA,; Volume 1, pp. 3–18.

Willmer C, Fricker M (1996) Stomata, Ed 2. Chapman and Hall, London

Zhao, B., C. Liu, J. Wang, et al. (2004). Spatial and temporal change of MODIS-NDVI in Xilinguole Grassland," Grassland of China, Vol. 26, No. 1, 1.

Zhang, L., H. Guo, C. Wang, L. Ji, J. Li, K. Wang, and L. Dai. (2014). The long-term trends (1982–2006) in vegetation greenness of the alpine ecosystem in the Qinghai-Tibetan Plateau. Environmental Earth Sciences 72:1827–1841

Zhang, X., Li, M., Ma, Z. et al. (2019). Assessment of an Evapotranspiration Deficit Drought Index in Relation to Impacts on Ecosystems. Adv. Atmos. Sci. 36, 1273–1287. https://doi.org/10.1007/s00376-019-9061-6

Zhang, Xiaoyang & Ni-Meister, Wenge. (2014). Remote Sensing of Forest Biomass. 10.1007/978-3-642-25047-7_3.